ISTANBUL TECHNICAL UNIVERSITY★GRADUATE SCHOOL

STRATIGRAPHY, GEOCHEMISTRY, AND PETROLOGY OF THE UPPER CRETACEOUS VOLCANIC ARC SEQUENCE NORTH OF ISTANBUL, WESTERN PONTIDES, NW TURKEY

M.Sc. THESIS

Cemre Ay

Solid Earth Sciences Department

Geodynamics Programme

JULY 2021

ISTANBUL TECHNICAL UNIVERSITY★GRADUATE SCHOOL

STRATIGRAPHY, GEOCHEMISTRY, AND PETROLOGY OF THE UPPER CRETACEOUS VOLCANIC ARC SEQUENCE NORTH OF ISTANBUL, WESTERN PONTIDES, NW TURKEY

M.Sc. THESIS

Cemre Ay
(602181010)

Solid Earth Sciences Department

Geodynamics Programme

Thesis Advisor: Doç.Dr Gürsel Sunal

JULY 2021

İSTANBUL TEKNİK ÜNİVERSİTESİ ★ LİSANSÜSTÜ EĞİTİM ENSTİTÜSÜ

İSTANBUL ZONU'NUN RİVA CİVARINDAKİ VOLKANİK KÖKENLİ ÜST KRETASE İSTİFİNİN STRATİGRAFİSİ, JEOKİMYASI, VE PETROLOJİSİ, BATI PONTİDLER KB TÜRKİYE

YÜKSEK LİSANS TEZİ

Cemre Ay
(602181010)

Katı Yer Bilimleri Anabilim Dalı

Jeodinamik Programı

Tez danışmanı: Doç. Dr Gürsel Sunal

TEMMUZ 2021

Cemre Ay, a M.Sc student of İTU Graduate School student ID 602181010, successfully defended the thesis/dissertation entitled "STRATIGRAPHY, GEOCHEMISTRY, AND PETROLOGY OF THE UPPER CRETACEOUS VOLCANIC ARC SEQUENCE NORTH OF ISTANBUL, PONTIDES, NW TURKEY", which she prepared after fulfilling the requirements specified in the associated legislations, before the jury whose signatures are below.

Thesis Advisor :	Assoc. Prof. Dr. Gürsel Sunal **İstanbul Technical University**	**.....**
Jury Members :	**Prof. Dr. Aral Okay** **Istanbul Technical University**	**.....**
	Prof. Dr. Namık Aysal **Istanbul University-Cerrahpaşa**	**.....**

Date of Submission : 11 June 2021
Date of Defense : 19 July 2021

FOREWORD

Firstly, I would like to express my sincere appreciation to my supervisor Doç. Dr. Gürsel Sunal for sharing his knowledge and experience with me during my master's thesis studies and encouraging me to improve myself with his patience and constructive criticism.

I also would like to express my sincere gratitude to Prof. Dr. Aral I. Okay not only for his constructive comments during my studies but also for his great help during my fieldwork.

I would like to express my sincere thanks to Prof. Dr Gültekin Topuz for helping me interpret my geochemical analysis and thin section studies and whose views I have benefited from throughout my thesis.

I would like to express my sincere thanks to Prof. Dr. Ercan Özcan for helping me with photographing and dating of the fossils in sandstones of İshaklı Formation.

I would like to express my sincere thanks to Prof. Dr. Timur Ustaömer for sharing his knowledge and opinions about my thesis and for always supporting me.

I would like to thank my dearest friend Ümitcan Erbil for always supporting me since my undergraduate life and sharing his ideas with me during my field studies.

I would like to thank my dear colleagues and friends, Res. Asst. İnal Demirkaya, Res. Asst. Ali Akın, Res. Asst. Ezgi Sağlam, Res. Asst. Turgut Duzman, Barış Tunçer, Hande Özcakmak, Eralp Bozkır, Res. Asst. Işıl Güraslan and Res. Asst. Yağmur Güneş for offering different perspectives and constructive feedback throughout my thesis.

I am grateful to my dear mother Elif Ay, my dear father Mehmet Ay, my dear brother Ozan Ay, my dear sister Rana Gün Ay and my dear niece Naz Ay for supporting me throughout my life and always being there for me.

This thesis was supported by İTÜ-BAP (MYL-2021-42902).

July 2021

Cemre Ay
(Geological Engineer)

TABLE OF CONTENTS

Page

ABBREVIATIONS

Cpx : Clinopyroxene

Fsp : Feldspar

GPS : Global positioning system

Hbl : Hornblende

HFSE : High field strength elements

HREE : Heavy Rare Eearth Element

LA-ICP-MS : Laser Ablation Inductively Coupled Plasma Mass Spectrometry

LILE : Large-ion lithophile elements

LOI : Loss on ignition

LREE : Light Rare Earh Element

Mg# : Magnesium number

OIB : Ocean island basalt

Pl : Plagioclase

Px : Pyroxene

PPL : Plane Polarized Light

Qtz : Quartz

REE : Rare earth element

TAS : Total Alkali Silica

Ves : Vesicular texture

XPL : Cross Polarized Light

LIST OF TABLES

Page

LIST OF FIGURES

Page

STRATIGRAPHY, GEOCHEMISTRY, AND PETROLOGY OF THE UPPER CRETACEOUS VOLCANIC ARC SEQUENCE NORTH OF ISTANBUL, PONTIDES, NW TURKEY

SUMMARY

The Upper Cretaceous volcanic arc belt extends along the southern coast of the Black Sea from Bulgaria in the west and to Iran in the east. The Istanbul Zone, in which the study area is located, is separated from the Sakarya Zone by the Intra-Pontide Suture in the south and from the Strandja Zone by the West Black Sea Fault in the west. The study area covers an area of approximately 330 km^2 on the eastern side of the Bosphorus.

The Upper Cretaceous volcanic units exposed roughly in E-W direction to the north of the Istanbul Zone are associated with a magmatic arc that developed as a result of the subduction of the Tethys ocean to the north, under the continental margin of Laurasia. The Upper Cretaceous volcanism continued its activity along the north of the Pontides in Turkey in the Turonian-Campanian interval. These volcanic units are clearly observed in the north of the Istanbul Zone, in the area from Anadolu Kavağı to the west of Şile. The Upper Cretaceous volcanic series are divided into two formations; İshaklı and Riva Formations.

The İshaklı Formation represents a fore-arc environment composed of volcanic sandstone, shale, siltstone, marl, tuff, and epiclastic rocks. The slump structures observed in the turbiditic sequence together with plant remains and a small number of coal formations in the sandstone indicating that the sediments were deposited in a fore-arc turbidite fan, most probably in front of a river delta. The Riva Formation consisting of andesitic-basaltic lavas, agglomerates, tuffs, and volcaniclastic rocks represents an arc / intra-arc environment and transitionally lies over the İshaklı Formation. The volcanic clasts in the Riva Formation are mainly angular and large. This indicates that the blocks were not transported far from the source area. Poorly lithified terrestrial sandstones and conglomerates unconformably overlie the volcanic units. The Upper Cretaceous volcanic units are overtrust by the Paleozoic sedimentary sequence along the Eocene Sarıyer-Şile Thrust Fault.

The trace elements of the volcanic rocks normalized to the primitive mantle show enrichment in lithophile elements with large ion diameters (LILE), while they show depletion in elements with low ion radius (HFSE). The relatively high ratio of LILE / HFSE and negative Nb, Ta, and Ti anomalies indicate that volcanism developed in a subduction environment. The results of geochemical analysis obtained during this study were compared with geochemical characteristics from the whole Upper Cretaceous arc belt in the Pontides to understand spatial and temporal relationship of the volcanism. Regional correlation suggests that the volcanism in the western part of the Istanbul Zone has similar geochemical features with that of the eastern Istanbul Zone and the Strandja Massif, but displays some differences with the Eastern Pontides and the Sredna-Gora Zone. On the other hand, geodynamic setting of the volcanism in the Istanbul region, shows close similarities with the Squanzi belt NW China which is interpreted as an intra-continental back-arc.

LA-ICPMS U-Pb zircon dating were performed on the tuff levels from the İshaklı and the Riva formations, which yielded 75.45±1.38 Ma (Middle Campanian) and 78.46±1.17-76.29±2.48 Ma (Lower Campanian), respectively. Paleontological data from the İshaklı Formation confirm these age results and indicate that the age of the İshaklı Formation is Middle-Upper Campanian. Stratigraphy, geochemistry and U-Pb ages obtained from the Upper Cretaceous volcanic rocks together with regional geological data compiled from the Pontides indicate that there was a transition during the Campanian from fore-arc to intra-arc setting when the Western Black Sea basin opened as a back-arc.

In the light of the information obtained, it is thought that there was a transition from the fore-arc turbiditic deposition to intra-arc volcanism in the Campanian period in the Istanbul Zone and the volcanism become younger was rejuvenated towards the west. The volcanic activity observed in the Campanian period in the Eastern Pontides and the Sredna-Gora Zone has high-K calc-alkaline and shoshonitic character. As a result of spatial and temporal correlation made with such regions of the Pontides showed that the calc-alkaline arc volcanism that formed as a result of the subduction of the Neo-Tethys ocean shifted to the high-K and shoshonitic character as a result of the opening of the Black Sea as a back-arc basin.

İSTANBUL ZONU'NUN RİVA CİVARINDAKİ VOLKANİK KÖKENLİ ÜST KRETASE İSTİFİNİN STRATİGRAFİSİ, JEOKİMYASI, VE PETROLOJİSİ

ÖZET

Üst Kretase yay volkanizması ürünleri batıda Bulgaristan'ın Sredna Gora Zonu'ndan başlayıp doğuda Gürcistan ve İran'a kadar uzanmaktadır. İnceleme alanının içinde bulunduğu İstanbul Zonu, güneyde Pontid-içi Kenedi ile Sakarya Zonu'ndan batıda ise Batı Karadeniz Fayı ile Istranca Zonu'ndan ayrılmaktadır. İnceleme alanı, İstanbul Boğazı'nın doğu yakasında ~330 km^2' lik alanı kaplamaktadır.

İstanbul Zonu'nun kuzeyinde D-B doğrultulu yüzlek veren Üst Kretase volkanik birimleri Tetis Okyanusu'nun kuzeye, Lavrasya kıta kenarı altına dalması sonucu gelişen magmatik bir yay ile ilişkilendirilmiştir. Üst Kretase Magmatik Yayı Türkiye'de Pontidler'in kuzeyi boyunca Turoniyen-Kampaniyen aralığında aktivitesini sürdürmüştür. Neo-Tetis Okyanusu'nun yitimine bağlı bu volkanikler İstanbul Zonu'nun kuzeyinde, Anadolu Kavağı'ndan Şile'nin batısına kadar olan alanda açık bir biçimde gözlenmektedir. Üst Kretase yayının ürünleri İstanbul Boğazın'nın doğu yakasında İshaklı ve Riva Formasyonu olarak ikiye ayrılmaktadır. İshaklı Formasyonu, volkanik kumtaşı, şeyl, siltaşı, marn, tüf ve epiklastik kayaçlardan oluşmaktadır. Kumtaşı içerisinde bitki kalıntıları ve az miktarda kömür oluşumları ile birlikte türbiditik istif içerisinde gözlenen kayma (slump) kıvrımları çökellerin bir yay-önü ortamda çökeldiğini işaret etmektedir. İshaklı Formasyonu üzerine geçişli olarak andezit-bazalt lavları, aglomeralar, tüf ve volkanoklastik kayalar ile yay/ yay-içi ortamını temsil eden Riva Formasyonu gelmektedir. Riva Formasyonu içerisinde bulunan blokların köşeli ve büyük boyutlara ulaşması, oluşan blokların kaynak alandan çok taşınmadığını ve oluşumundan sonra bölgenin yükseldiğini göstermektedir. Üst Kretase volkanik birimleri Eosen yaşlı bir bindirme fayı ile Paleozoik sedimenter istifi tarafından üzerlenmektedir. Bu istiflerin üzerine uyumsuz olarak karasal çökelme ortamını yansıtan kumtaşı ve çakıltaşından oluşan Neojen yaşlı bir istif gelmektedir. Riva Formasyonu içerisinden alınan lav ve

aglomera örnekleri üzerinde tüm-kaya jeokimya analizleri yapılmış ve ana oksit, iz element ve nadir toprak element konsantrasyonları ölçülmüştür.İstanbul Zonun'da gerçekleşen volkanizma, düşük-K kalk-alkalen, orta-yüksek K kalk-alkalen kimyasal özellineğe sahiptir. Analiz edilen örneklerin magnezyum numaralı 32%-51% arasında değişkenlik göstermektedir. İlkel mantoya göre normlaştırılan iz elementler, geniş iyon çaplı litofil elementlerce (LILE) zenginleşme gösterirken düşük iyon yarıçapına sahip elementlerce (HFSE) fakirleşme gösterirler. LIL/HFS oranının görece yüksekliği ve negatif Nb, Ta ve Ti anomalileri göstermeleri volkanizmanın bir yitim ortamında geliştiğini işaret etmektedir (Pearce and Peate, 1995).

Pontidler'in kuzeyi boyunca yüzeylenen Üst Kretaseye ait volkanik birimlerin jeokimyasal analiz sonuçları, İstanbul Zonu'nda yüzeylenen volkanik birimler ile volkanizmanın zaman ve mekan içinde değişimini ortaya koymak amacı ile karşılaştırılmıştır. Karşılaştırmalar sonucu inceleme alanında gerçekleşen volkanizma ile Istranca ve İstanbul Zonu'nun doğusunda gerçekleşen volkanizma karakteri benzerlik göstermektedir.

Doğu Pontidler ve Sred-Gora Zonu'ndan derlenen analiz sonuçları ise inceleme alanında gerçekleşen volkanizmanın farklılaşması sonucu uyumsuz elementlerce daha fazla zenginleşme gösterirken uyumlu elementlerce daha fazla tüketildiği göstermektedir. İstanbul bölgesinde gerçekleşen volkanizmanın jeodinamik ortamını hakkında yorum yapabilmek için bu çalışma kapsamında yapılan jeokimya analizleri kıta-içi yay arkası (intra-continental back-arc) olarak yorumlanan farklı alanlarda yüzeylenen volkanik kayaların kimyası ile karşılaştırılmıştır. Bu çalışmanın jeokimya analiz sonuçları kıta-içi yay arkasında (intra-continental back-arc) meydana gelen volkanizmanın kimyası ile uyumluluk göstermektedir. Bu çalışma sonuçlarına göre elde edilen La/Yb: 4.42-7.25 Ba/La: 16.40-43.87 Sm/Nd: 0.22-0.25 değerleri Jiang ve diğ.,(2017) tarafından ileri sürülen tipik kıta-içi yay ardı ortamını temsil eden $(La/Yb)_N > 3$, $Ba/La > 10$ and $Sm/Nd < 0.3$ değerleri ile uyumluluk sağlamaktadır.

İshaklı ve Riva Formasyonu içerisinde tüf seviyelerinden U-Pb zirkon analizi için örnek alınmıştır. U-Pb zirkon yaşları sırasıyla 75.45 My (Orta Kampaniyen) ve 78.46-76.29 My (Alt Kampaniyen) olarak belirlenmiştir.

Pontidlerin kuzeyi boyunca yapılan eski çalışmalar sonucu İshaklı Formasyon'unun (Dereköy) yaşı paleontolojik veriler ile Turoniyen-Santoniyen olarak belirlenmiştir.

İshaklı Formasyonu içersinde kumtaşlarından hazırlanan ince kesitler içerisinde *Globotruncanita cf. elevata* (Brotzen), *Globotruncana cf. arca* (Cushman) *ve Globigerinelloides sp.* fosilleri tespit edilmiştir. Bu fosiller İshaklı formasyonunun Kampaniyen döneminde çökeldiğini işaret etmektedir. Paleontolojik ve U-Pb zircon yaşlandırma sonuçları birbiri ile uyum göstermektedir.

Bu çalışma sonuçlarına göre Üst Kretase volkanizması, İstanbul Zon'unun kuzeyinde U-Pb zirkon yaşları ve paleontolojik verilere göre Kampaniyen döneminde aktivitesini sürdürmüştür. Elde edilen bilgiler ışığında İstanbul Zonun'da Kampaniyen döneminde yay-önü türbiditik ortamından yay/yay-içi volkanizmaya geçiş olduğu ve volkanizmanın batıya doğru gençleştiği düşünülmektedir. Doğu Pontidlerde ve Sredna-Gora zonunda Kampaniyen döneminde gözlenen volkanizma yüksek-K kalk-alkalen ve şoşonitik karaktere sahiptir.

Bu çalışma verileri ile yapılan karşılaştırmalar sonucu Tetis okyanusunun yitimi ile gerçekleşen kalk-alkalen yay volkanizması Karadeniz'in bir yay-ardı havza olarak açılması sonucu volkanizmanın karakterinin yüksek-K ve şoşonitik karaktere geçiş yaptığını işaret etmektedir.

1. INTRODUCTION

1.1 Geographic location

The study area, which covers an area of ~330 km^2 is located in Anadolu Kavağı to the west of Şile region, east of Bosporus (NW Turkey), and bordered by the Black Sea in the north (Fig. 1.1).

Figure 1.1: The location of the study area.

1.1.1 Geography

The Riva Stream alligned roughly NW / SE direction is located in the study area, which flows starting from Kocaeli province to the Black Sea from the village of Riva. Some of the other geographical elements in the region are 201 m high Yuşa hill, and Fil Capes, Poyraz Capes, Kelağra Capes and Döşeme Capes that are formed as a result of small protrusions made by the land to the sea.

Figure 1.2: 3D digital elevation model of the study area

1.1.2 Climate and vegetation

Because the study area is located in the Black Sea coast it has a typical Black Sea climate, temperature is mild in the winters and cold in the summer seasons. In addition to having a warm and temperate climate, the Mediterranean and the Black Sea climates follow each other in the region. The annual average temperature of the region is 14.1 °C and the annual average rainfall is about 747 mm. In winter, there is much more rainfall in İstanbul than in summer.

1.2 Aim and Method of the Study

The aim of this study is to determine the formation environment, stratigraphy, start of the magmatism and evolution of the Upper Cretaceous magmatic arc belt outcropping in the north of the Istanbul Zone. Within the scope of this study, detailed geological map of 1/25.000 of the region was prepared and petrographic and paleontological studies, U-Pb zircon dating and geochemical analysis were performed. Silva type compass, GPS, topographic maps, hand-lens and geological hammer were used in the field study. To reveal petrography of the volcanic and volcanoclastic rocks of the Upper Cretaseous volcanic arc, 25 thin sections were investigated.

1.2.1 LA-ICP-MS zircon dating

Zircon minerals were separated from 4 volcanic rock samples. After the rocks were crushed by hydraulic press, their grain sizes were reduced by cylindrical grinding. Then, 63-180 and 180-250 micron grains were separated using a sieve machine. The separated sample was passed through a magnetic separator and the nonmagnetic part was obtained. The sample was then floated in heavy liquid (Sodium Polytungstate) and minerals with a density greater than 2.85 g/cm^3 precipitated. Then, under the microscope, zircon grains were selected with tweezers and adhered to the band. A ring was prepared by pouring epoxy on zircon grains. The surfaces of the zircon grains were polished and electron microprobe images were taken.

Zircon separation processes were done at the Istanbul Technical University, Eurasia Institute of Earth Sciences, Sample Preparation, and Mineral Separation Laboratory. Zircon minerals were dated at the Istanbul University-Cerrahpaşa, Geochronology and Geochemistry Laboratories in İstanbul. Zircon U-Pb analyses were conducted by using Perkin Elmer NexION 2000 ICP-MS combined with the ESI NWR-213 solid phase laser (İskenderoğlu and Aysal, 2021). Spot size of the zircon grains vary between 25 and 40 micron, and Helium was used as carrier gas (0.5 l/sec) (İskenderoğlu and Aysal, 2021). Zircon reference material 91500 was selected as a primary standard, and AusZ-10 (38 Ma) and MudTank (750 Ma) as secondary reference materials (İskenderoğlu and Aysal, 2021).

1.2.2 Whole-rock geochemistry

Whole-rock geochemistry was conducted on 6 volcanic rocks within the Riva Formation. The rocks were first crushed by hydraulic press and then reduced to size with a cylindrical grinder. Then the samples were powdered with a vibrating disc grinder. ICP-AES and ICP-MS were used for whole-rock geochemistry analysis of the samples at the Bureau Veritas Mineral Laboratories in Ankara, Turkey. Reference Material STD SO-17 were used for calibration in the analysis of the samples.

1.3 Previous studies

Okay et al. (1994) found that two oceanic basins belonging to the Black Sea were separated by the Middle Black Sea Rift. They claim that the Western Black Sea

Basin was opened as a result of northward subduction of the Intra-Pontide ocean during the Aptian-Cenomanian through rifting of the Istanbul Zone from the Odessa Shelf. The development of the Black Sea ended in the Early Eocene as a result of collision between the Istanbul and Sakarya Zone. After the collision, compressional structures (thrusts) developed along the shores of the Black Sea, the Miocene faulting in the Karkinitsky basin, and the south of the Greater Causcaus basin.

Tüysüz (1999) reported that there are two different sedimentary basins on two different tectonic units developed during the Cretaceous tectonic evolution of the region in the Pontides. As a result of the studies based on the Istanbul Zone and the Sakarya Zone, he postulated that there are differences in the stratigraphy of the zones before the Upper Cretaceous. He stated that the data he obtained support the work of Okay's (1994) idea that the Istanbul Zone was a part of the Odessa Shelf just before the beginning of arc magmatism and took its present location sometime in the Early Eocene.

Keskin et al. (2003) defined the Upper Cretaceous volcanic sequence as the Kavaklar Groupin the west of İstanbul Zone. From bottom to top, the volcanic sequence is the Bozhane, Garipçe and Kısırkaya Formations, respectively. Based on geochemical characteristics of the lavas and dykes, they determined that the Garipçe Formation has a calc-alkaline nature with subduction component whereas the Kısırkaya Formation has an alkaline, within-plate component. As a result of stratigraphic and geochemical studies, it was interpreted that the Kavaklar Group did not show the typical stratigraphy of the magmatic arc and presence of the syn-sedimentary faults and neptunian dykes in the sequence were interpreted as that it formed in an extentional tectonic regime during its deposition. Thus, they indicated that the Kavaklar Group was deposited as a continental margin as a result of the rifting of the Istanbul Fragment and the Western Black Sea Basin was opened as an intra-arc / back-arc environment.

Gedik et al. (2005) They made a detailed geological map of the Upper Cretaceous succession in İstanbul Zone. They named the Upper Cretaceous succession as the İsaklı and Riva formations. They stated that these units have lateral and vertical transitions. The age of the Ishaklı formation was determined as Santonian-Campanian based on paleontological data.

Yavuz (2008) separated the Upper Cretaceous volcanic rocks of the Istanbul zone according to their facies both in the east and west sides of the Bosphorus. The volcanic units are described from bottom to top Bozhane, Sarıyer, Garipçe, and Kısırkaya Formations, respectively. As a result of petrographic and geochemical analyzes of volcanic rocks, he claimed that volcanism arose not from a single volcanic vent, but from many parasitic vents. K-Ar dating and fossil findings indicate that volcanism in the Istanbul Zone lasted until the Maastrichtian period.

Tüysüz et al. (2012) examined the Unaz Formation that separates two different volcanic units in the Zonguldak area. They stated that in the first stage of volcanism, volcanic units and sedimentary rocks were formed under the effect of a extentional tectonic regime in the late Cenomanian-Turonian-Santonian period along the horst-graben structures that were formed in the southern Black Sea basin under the extensional stress regime. The extensional period was interpreted as rifting of magmatic arc and opening of the Western Black Sea Basin as an intra-arc/back-arc basin. They suggested that there was a rapid subsidence followed by rifting in the southern part of the Black Sea during the Late Cenomanian. In this period, with the termination of volcanism, the pelagic limestones of the Upper Santonian Unaz Formation was deposited along the horst and graben areas. This event has been interpreted as the beginning of oceanic spreading in the Western Black Sea Basin. What they indicated that the Unaz formation is underlain by the Dereköy Formation in the grabens while there is no Dereköy formation in the horst areas.

Yılmaz Şahin et al. (2012) studied the Çavuşbaşı Granodiorite located north of the Istanbul Zone in the Western Pontides. The Çavuşbaşı intrusion consists of granodiorite, tonalite and partially quartz diorite. They obtained ages of 67.91 Ma and 67.59 Ma zircon U-Pb ages from samples taken from intrusion. Hornblende and biotite minerals yielded K-Ar age of ~63 Ma. As a result of petrography and geochemical studies, the Çavuşbaşı Granodiorite was defined as an adakitic intrusion formed in Upper Cretaceous interval. They suggested that the Çavuşbaşı Granodiorite was formed by partial melting of the submerged oceanic slice under the conditions of amphibolite-eclogite facies as a result of the northward subducted of the northern branch of the Neotethys ocean along the İzmir-Ankara and Intra-Pontide suture.

Keskin and Tüysüz (2018) defined two different magmatic series according to geochemical analysis in the Upper Cretaceous volcanic units developed on the central and western Pontides. They reported that the magmatism that took place in the first stage derived mainly from the depleted mantle source associated with the extensional tectonic regime as a result of the subduction of the northern branch of the Tethys ocean along the south of the Laurasian Continent and has also a subduction component. They argued that second stage magmatism derived from both the depleted mantle source and the enriched astenospheric mantle source which similar to Ocean Island Basalts. Interpreting the geochemical, stratigraphic, paleontological and sedimenter data, they suggested that the northern part of the Black Sea was opened as a back-arc / intra-arc basin between Turonian and Santonian. The magmatics cutting the Paleozoic rocks were defined as lamproite and diabase dykes, intermediate intrusions and granodioritic stock and sub-volcanics. The Calk-alkaline mafic-intermediate dykes have a clear subduction component, while alkali dykes and lamproite dykes are anorogenic and within-plate alkaline in nature. As a result of the studies carried out, they suggested that the dyke complexes found in the Istanbul Zone were related to the volcanic arc that was rifted with the opening of the Black Sea during the Late Cretaceous-Paleocene interval.

Aysal et al. (2018) studied geochemistry of mafic-intermediate dykes and intrusions exposed in the northern part of Istanbul. They suggest that mafic dyke complex show calc-alkaline/alkaline characteristics, but intermadiate dykes have alkaline composition. They concluded that calc-alkaline mafic and intermediate have a subduction component whereas the alkaline rocks including lamproites have formed in an anorogenic environment. They indicated that the formation of these different dyke complexes is associated with opening of the Black Sea during the Late Cretacous-Paleocene.

Boehm et al. (2019) They obtained two different ages from nanofossil and planktic foraminifera in pelagic sedimentary units interbedded with the Upper Cretaceous volcanic rocks. The age of the Dereköy Formation at the base was determined as Turonian-Santonian, while the age of the Cambu Formation overlying the Dereköy Formation was determined as Lower-Middle Campanian. Based on geochemical results, they stated that the volcanic series display calc-alkaline to shoshonitic character and this indicates a volcanic arc setting.

1.4 Geological Setting

Turkey which is a part of the Alpine Orogenic Belt, represents geologically a quite complex region where continental collision, subduction-accretion and obduction events are common (Şengör and Yılmaz, 1981; Okay and Tüysüz, 1999). Turkey is composed of three major tectonic units (Figure 1.3). These are the Pontides, the Anatolide-Tauride Block and the Arabian Platform (Ketin, 1966). These tectonic units became a single landmass along suture belts after the closure of the Tethyan oceanic branches starting from Oligocene in the north and west and the Oligo-Miocene periodin SE (Şengör and Yılmaz, 1981; Okay and Tüysüz, 1999). Pontides are made up of three tectonic zones. These are the Strandja Massif, the Istanbul, and the Sakarya Zones (Okay and Tüysüz, 1999). The Pontides and the Anatolide-Tauride block are separated by the Izmir-Ankara-Erzincan suture zone, which is thought to have been formed as a result of the closure of the Tethys ocean (Şengör and Yılmaz, 1981; Okay and Tüysüz, 1999).

Some researchers have suggested that Sakarya and Istanbul regions came together as a result of the closure of the Intra-Pontide ocean, which is thought to be the northern branch of the Tethys ocean, during the Early Eocene time (Akbayram et al., 2016).

The Istanbul Zone was located in south of the Odessa shelf until the Early Cretaceous period and the Western Black Sea Basin opened behind it as a result of the rifting of the Istanbul-Moesia continent when in the south, in the same period the Intra-Pontide ocean was subducting northward (Okay et al., 1994).

The Istanbul Zone, in which the study area is located, starts from Çatalca in the west and extends for 400 km to Araç-Daday-İnebolu in the east (Okay, 2008).

The Istanbul Zone is tectonically bounded with the Sakarya Continent in the east by the West Black Sea Fault and by the Intra-Pontide Suture in the south.

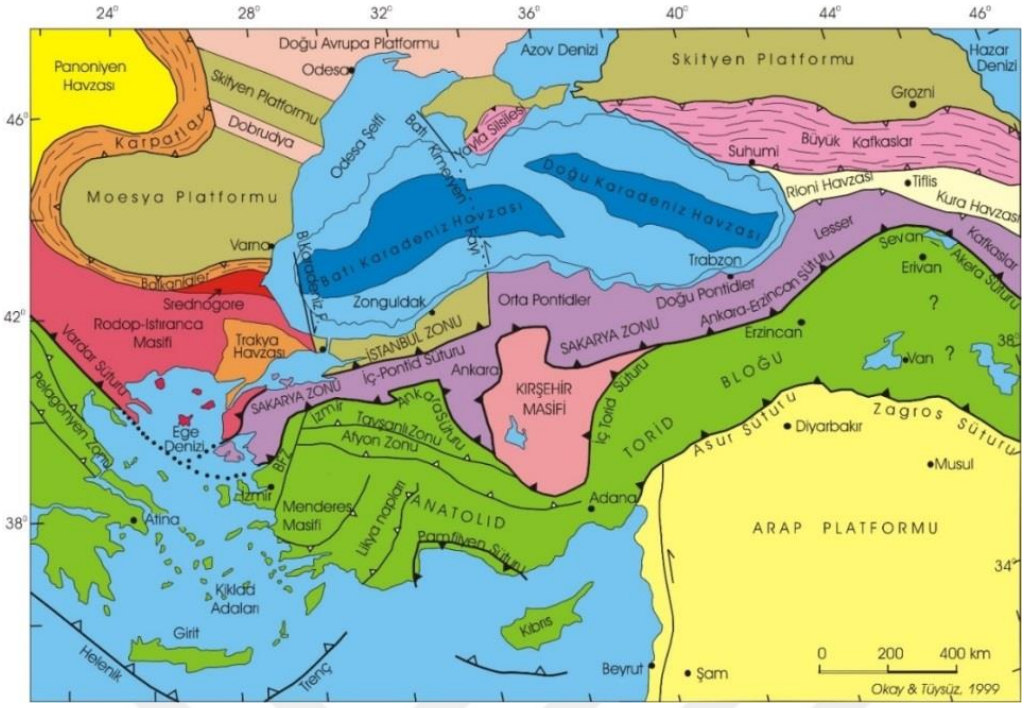

Figure 1. 3: Tectonic map of the Eastern Mediterranean region showing the main tectonic units and suture zones in Turkey (Okay and Tüysüz, 1999).

1.4.1 Istanbul Zone

The basement of the Istanbul Zone starts with high metamorphic and magmatic rocks (Chen et al. 2002; Yiğitbaş et al. 2004; Ustaömer et al. 2005). The well developed sedimentary sequence of Ordovician-Carboniferous age nonconformably overlies the basement rocks (Görür et al. 1997). The Paleozoic sequence begins with the arcosic series representing the river and lake environment and continues with Silurian, alternating siltstone and shale deposits representing the beach environment (Sayar,1979; Önalan,1982). A thick carbonate sequence, representing the transition from the shallow to deep marine environment of the Silurian-Devonian age lies on this sequence. The carbonate sequence passes up into a flysch sequence composed of Lower Carboniferous sandstone-shales. The Paleozoic sequences were deformed during Carboniferous as a result of Variscan orogeny and then intruded by Permian granitoids (Bürküt, 1966; Yılmaz, 1977; Yılmaz-Şahin et al. 2010; Aysal et al. 2018b). The east and west of the Istanbul Zone show different stratigraphies. In the Carboniferous, the western Istanbul Zone consists of deep marine turbitides, while in the east there are coal and shallow marine sediments. The sequence in the west of the Istanbul Zone is similar to the North West European stratigraphy (Okay et al., 2006). At the top of the sequence there is a Triassic transgressive rocks representing the

deepening environment (Okay et al., 2006). The Triassic sequence consists of terrestrial conglomerate, sandstone, and mudstone (Altınlı, 1968; Yurtsever, 1982). While the Triassic succession is unconformably overlain by the Jurassic shallow marine limestones and the Jurassic sequence is unconformably overlain by the Lower Cretaceous flysch sequence (Figure 1.4) in the east of the İstanbul Zone (the Zonguldak Zone), the Jurassic and Lower Cretaceous sequence are absent in the west of the İstanbul Zone (Okay et al., 2006). In the western part of the Istanbul Zone, the Triassic sequence is unconformably overlain by Upper Cretaceous volcanic units (Okay et al., 2006).

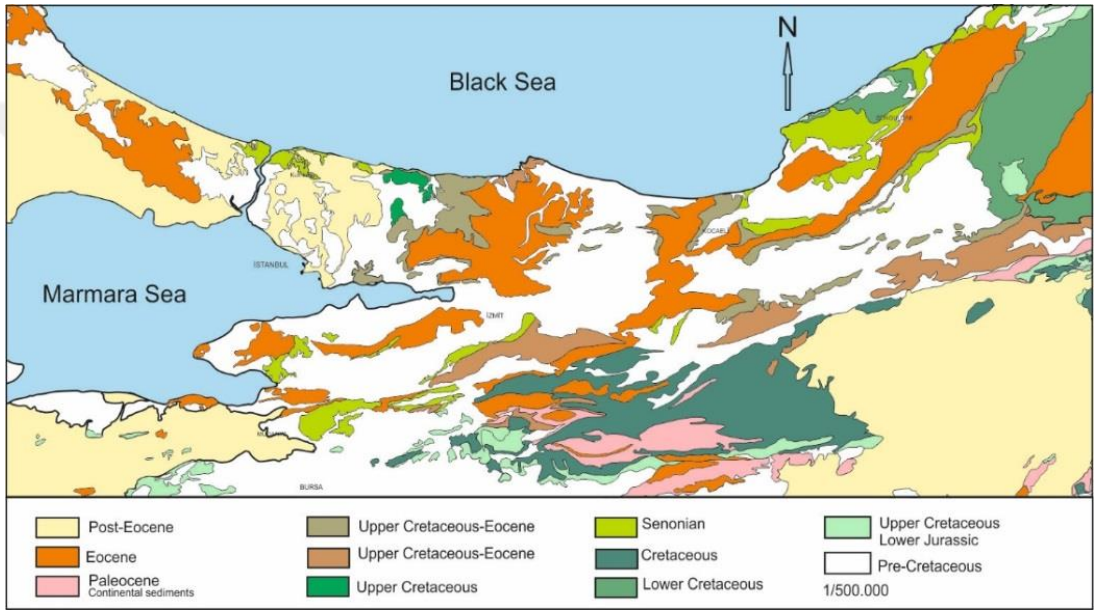

Figure 1.4: Simplified geological map of NW Turkey showing the Cretaceous outcrops.

1.4.3 Cretaceous Magmatic Arc

The Sakarya and Istanbul Zones are separated by the Intra-Pontide ocean, which was thought to be one of the northern branch of the Tethyan oceans (Şengör and Yılmaz., 1981). The Sakarya and Istanbul Zones collided in the Early Eocene time (Akbayram et al., 2016). Due to subduction of the oceanic crust under the Pontides, the Upper Cretaceous volcanic arc formed on the northern part of the whole Pontides extending from Georgia to the Sredna-Gona Zone of Bulgaria (Georgiev et al., 2009) (Figure 1.5).

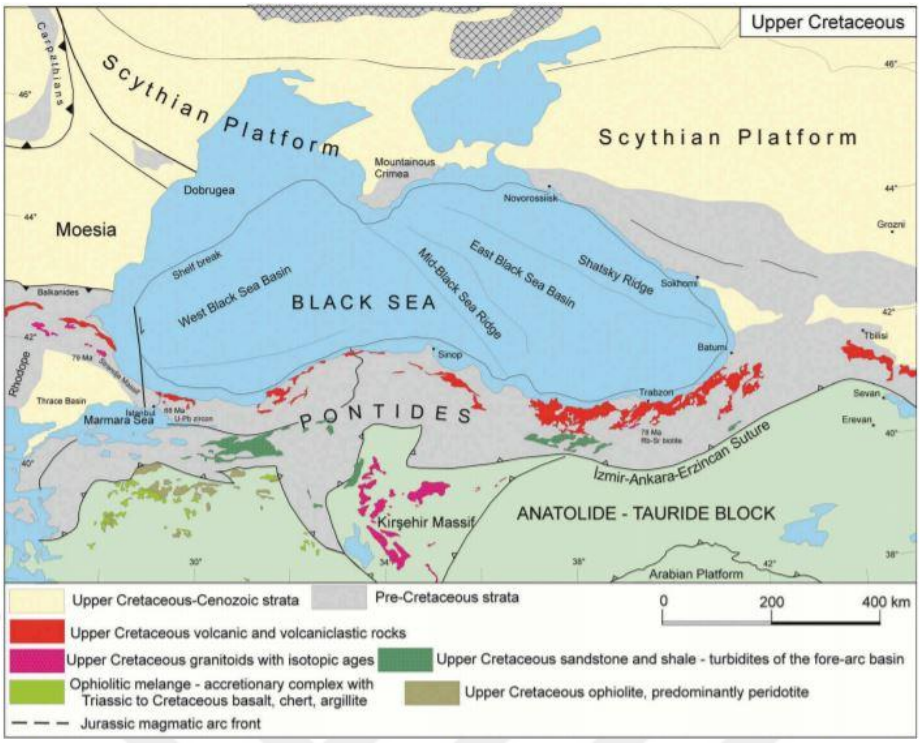

Figure 1. 5: Map showing the distribution of the Upper Cretaceous arc related magmatic rocks (Okay and Nikishin, 2015).

In the first stage, as a result of the subduction of the Tethys ocean under the Pontides' continental crust and the initiation of extensional tectonism, magmatism occurred as a calc-alkaline character with pronounced subduction signature. This early stage magmatism ended up with the deposition of the deep marine limestones of Upper Santonian age, and then the second stage magmatism started in the Campanian (Tüysüz, 2012; Keskin and Tüysüz., 2017).The presence of deep marine sediments marks the initiation of the Western Black Sea ocean spreading. Volcanism, which exhibits a calc-alkaline composition in the early products of the second stage volcanism, passes to alkaline chemistry towards its final stages. This change in the composition of the volcanism is interprated by some researchers as the change of the tectonic regime from subduction to extensional regime (Keskin and Tüysüz., 2018; Aysal et al. 2018a). The calc-alkaline magmatism occurred in the first stage, and then a back-arc rifting occurred as a result of the roll-back of the slab, and the magma character turned to alkaline (Keskin et al., 2010; Keskin and Tüysüz., 2018; Aysal et al. 2018a). This change in composition of Upper Cretaceous magmatism in the north of the Istanbul Zone is interpreted as the formation of astenospheric alkaline magmatism as a result of pressure melting with the thinning of the lithosphere (Keskin et al., 2010).

2. STRATIGRAPHY OF THE STUDY AREA

The stratigraphy of the study area is represented from bottom to top by Paleozoic sequence, Upper Cretaceous volcanic-volcanoclastic series, and Neogene deposits that unconformably cover all of the rock below.

The Paleozoic sequence was deformed during the Carboniferous period as a result of Variscan orogeny. The sequence crops out in the south of the study area and tectonically overlies the Upper Cretaceous volcanic series along a well-known thrust fault called as Sarıyer-Şile thrust Fault (Akartuna, 1963; Baykal and Önalan, 1980; Özgül, 2012; Baykal, 1943).

The volcanic series in the study area is divided into two formations; the İshaklı Formation and the Riva Formation. The equivalents of the Upper Cretaceous volcanic series in the east of the Istanbul Zone are separated by the Unaz formation representing Upper Santonian pelagic limestones (Tüysüz et al., 1999; Sunal and Tüysüz, 2002). However, in the study area, pelagic limestones are not observed between the two volcanic series, instead these series show a gradual contact with each other.

The İshaklı Formation consists of a turbiditic sequence representing the fore-arc environment, while the Riva Formation consists of andesitic-basaltic lavas and agglomerates representing the arc/intra-arc environment. These two formations have a transitional contact with each other and are unconformably overlain by the Neogene deposits covering most of the study area.

The geological map of the study area was prepared within the scope of this study and observation points, and sample locations collected for U-Pb dating and geochemistry analysis were indicated on the map (Figure 2.1). Generalized stratigraphic section of the study area is given in Figure 2.2.

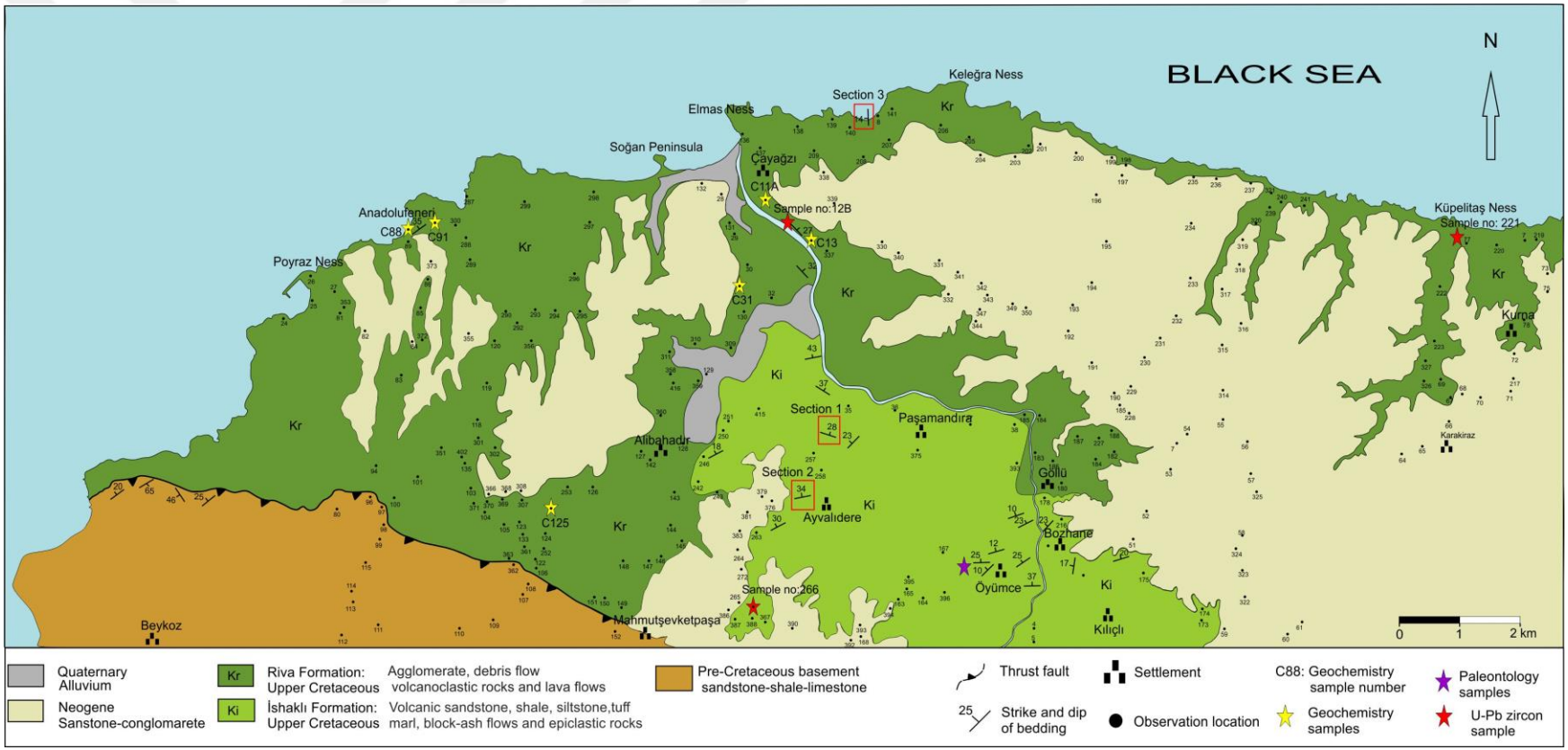

Figure 2. 1: The geological map of the study area. Red stars indicate locations of rocks collected for U-Pb zircon dating. Yellow stars indicate locations of rocks collected for geochemical analysis.

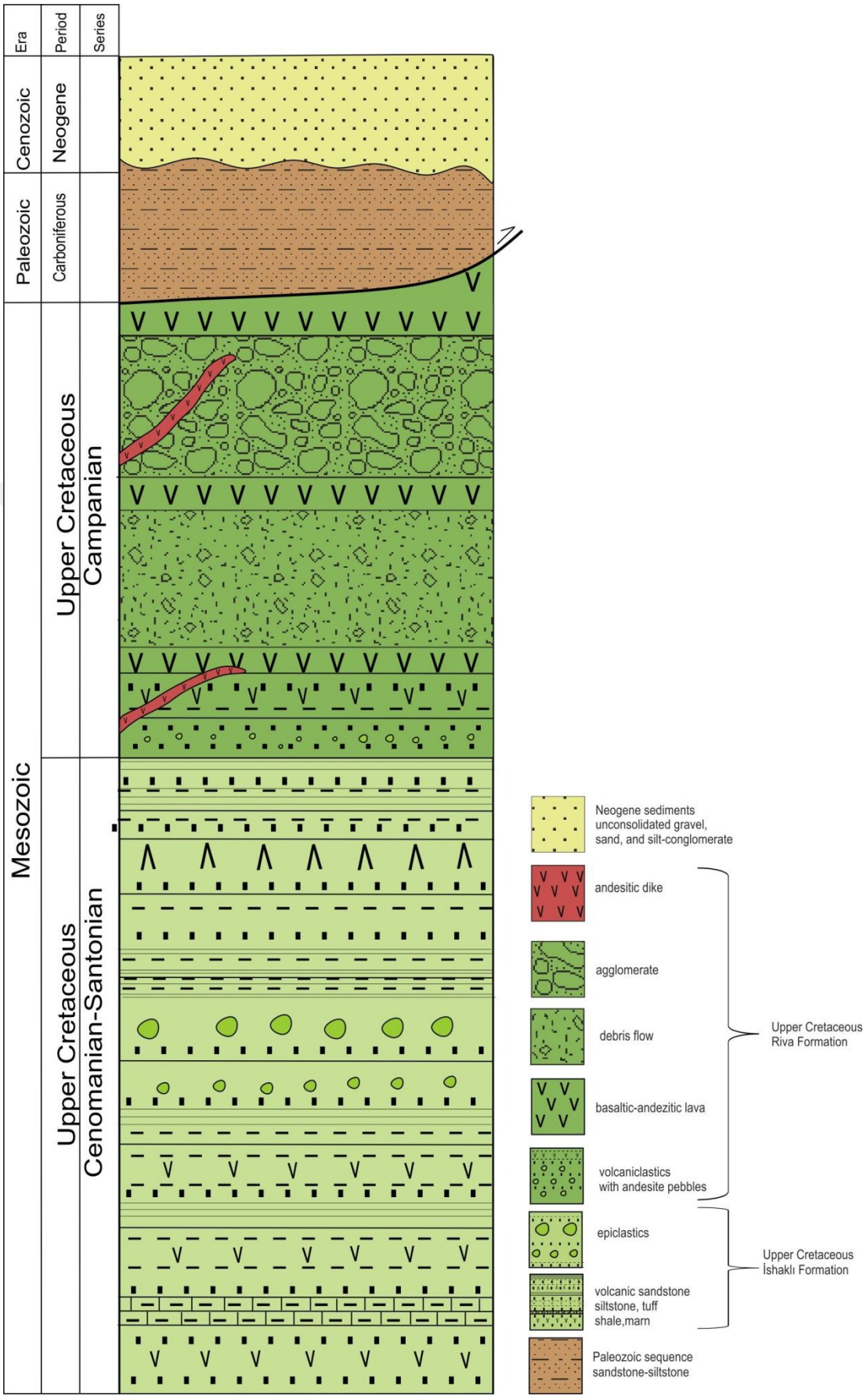

Figure 2. 2: Generalized stratigraphic section of the study area

2.1 The Paleozoic Sequence

The Paleozoic sequence consisting of sandstone, siltstone, and shales was first named by Penck (1919) as the Trakya Series. In later studies, the sequence was named the Trakya formation by Kaya (1971). It covers a region in the study area approximately 14 km long and 4 km wide.

It is observed that the sandstones in the study area are interbedded with siltstone and shale layers. Siltstones and shales are laminated, while sandstones are medium-thick bedded (Figure 2.3a). The age of the succession was determined as Lower Carboniferous according to paleontological data (Kaya 1971). The Paleozoic succession tectonically overlies the Upper Cretaceous volcanic unit along with the Şile-Sarıyer thrust Fault (Akartuna, 1963; Baykal and Önalan, 1980; Özgül, 2012; Baykal, 1943) in the south of the study area. Towards the thrust fault, the sequence is folded and there is steepening in the layers (Figure 2.3b).

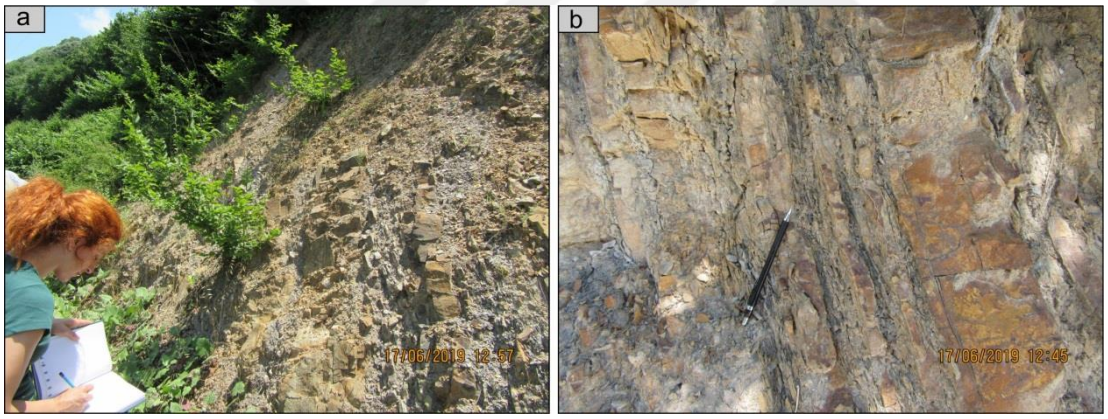

Figure 2.3: Field photographs of the Paleozoic sequence. a) sandstone-shale intercalation b) medium-bedded steeping sandstones.

2.2 Upper Cretaceous Volcanic-Volcanoclastics

While the Upper Cretaceous volcanic sequence was first named as Yemişliçay Group by Ketin and Gümüş (1963), Keskin et al. (2003) renamed it as the Kavaklar Group. In this study, the Upper Cretaceous rocks will be called as the İshaklı and the Riva formations as distinguished by Gedik et al. (2005).

2.3 The İshaklı Formation

The İshaklı Formation consists of volcanic sandstone, shale, siltstone, marl, and epiclastic rocks. Its equivalent sections were previously named as the Dereköy Formation by Şahintürk and Özçelik (1983) and the Bozhane Formation by Keskin et al. (2003). The İshaklı Formation crops out in Bozhane, Öyümce, south of Paşamandıra, south-east of Ayvalıdere and Kılıçlı villages in the study area. It covers a region in the study area approximately 7 km long and 5 km wide.

The volcanic sandstones are green, gray, yellowish brown and reddish. The volcanic sandstones exhibit pronounced exfoliation in the study area, which are generally well bedded and locally altered (Figure 2.4c). Shale and siltstone are thinly bedded and laminated. Marl and silicic tuff levels are observed in the turbidite sequence in the east of Bozhane village. In the study area, slumps with related folds are observed in siltstone-shale intercalation (Figure 2.4b). Siltstone-shale intercalation can be observed on the outcrops along the road-cuts of the Yavuz Sultan Selim Bridge and the Northern Marmara Highway (Figure 2.4a, d).

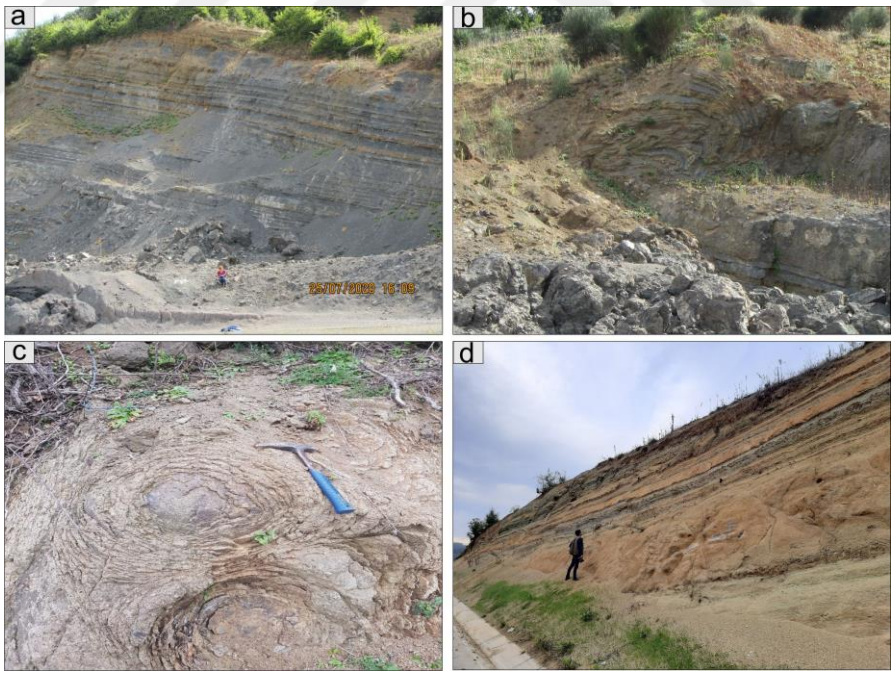

Figure 2.4 : Field photographs of the İshaklı formation. a)The turbiditic sequence composed of siltstone and shale intercalations. (on Northern Marmara Highway), b) slump flow / folds are observed in siltstone-shale intercalation (on Northern Marmara Highway), c) volcanic sandstones which exhibit well developed exfoliation. (on Northern Marmara Highway), d) The turbiditic sequence composed of siltstone, sandstone and shale intercalations. (on Northern Marmara Highway).

Measured stratigraphic sections from the Ishaklı Formation were studied along the different locations in the study area (Figure 2.10). The Ishaklı Formation begins with both fine-grained and coarse-grained reverse graded clastic rocks and passes up tuffs, epiclastic rocks and debris flow horizons. There is a normal graded clastic series in the upper part of the Ishaklı Formation (Figure 2.6b).

Epiclastic rocks have well-rounded and poorly sorted blocks and pebbles. it is surrounded by a clastic matrix. (Figure 2.5d). Debris flows consist of block and ash flow deposits (Fig. 2.5c). The blocks are composed of volcanic and volcaniclastic rocks. Some blocks show well-developed exfoliation structures because of weathering. The tuffs within the İshaklı Formation are composed of lithic tuffs (Figure 2.5b and Figure 2.6d) and crystalline tuffs (Figure 2.6c). A small amount of coal formation (Figure 2.7c,d) together with plant remains in the volcano-sedimentary sequence indicate that this sequence was formed as a result of turbiditic flows in front of the delta mouth. Slump structures, debris flows, marl, and pelagic fossils observed in the turbidite sequence indicate that the İshaklı formation was deposited in a fore-arc basin.

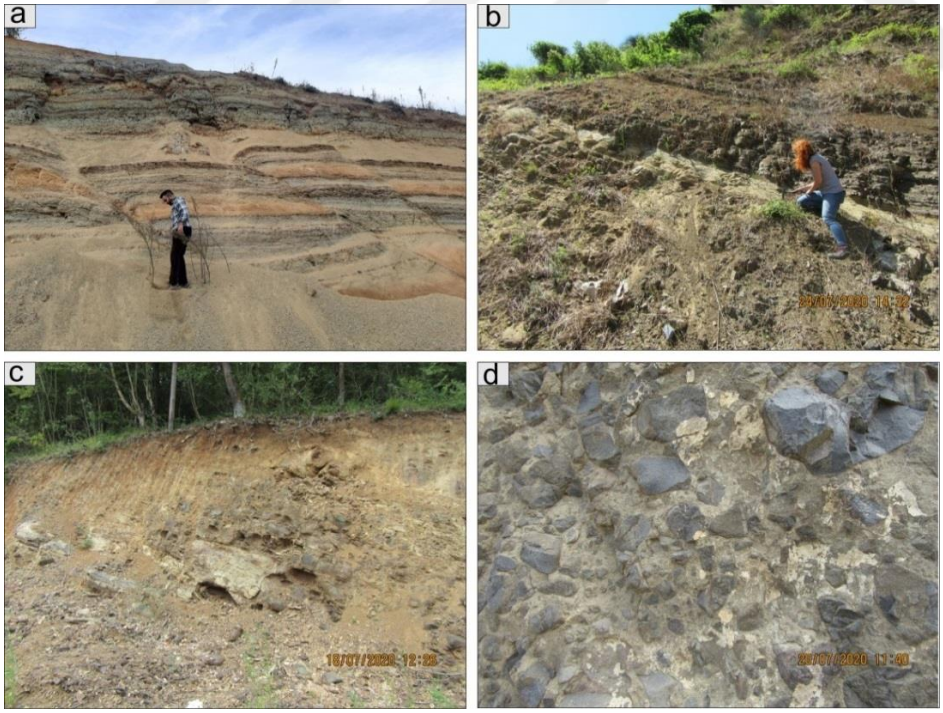

Figure 2.5 : Field photographs of İshaklı formation. a) Turbiditic succession cut by normal faults on Northern Marmara Highway, b) Volcanic sandstone and lithic tuff intercalation. (Değirmendere), c) debris flow over interbedded sandstone and siltstone (Ayvalıdere), d) epiclastic rocks composed of volcanic and sedimentary blocks.

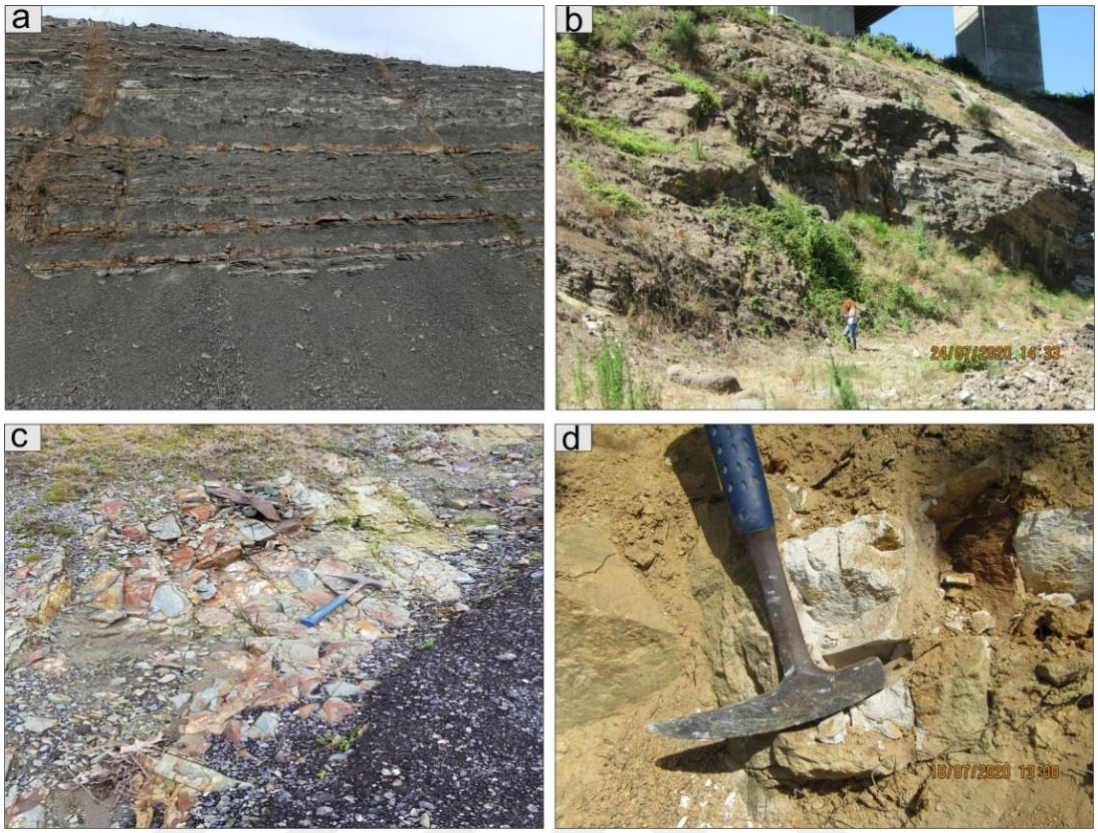

Figure 2. 6 : Field photographs of İshaklı formation. a) siltstone-shale intercalation within the turbiditic sequence, b) The volcanoclastic sequence forming the İshaklı formation, c) fine-grained silicic tuff d) acidic tuff level within the İshaklı formation.

The lithic tuff levels within the İshaklı Formation are composed of volcanic rock fragments, euhedral-subhedral amphibole, and plagioclase minerals. The tuff sample composed of fine-grained plagioclase and quartz minerals (Figure 2.7a,b).

Volcanic sandstones contain anhedral feldspar and quartz minerals also volcanic rock fragments. The plagioclase minerals display zoning and sieve texture. Occasionally, muscovite minerals are observed in thin sections. Volcaniclastic blocks within the debris flow display zoned plagioclase, clinopyroxene minerals, and volcanic rock fragments. The plagioclase minerals exhibit polysynthetic twinning and sieve texture.

The age of the İshaklı Formation according to nannoplankton and planktic foraminifera was determined as Upper Santonian-Campanian (Gedik et al., 2005). The Dereköy formation, which is the equivalent of the İshaklı formation in the east of the Istanbul zone, has been paleontologicaly determined as Upper Turonian-Santonian (Boehm et al., 2019).

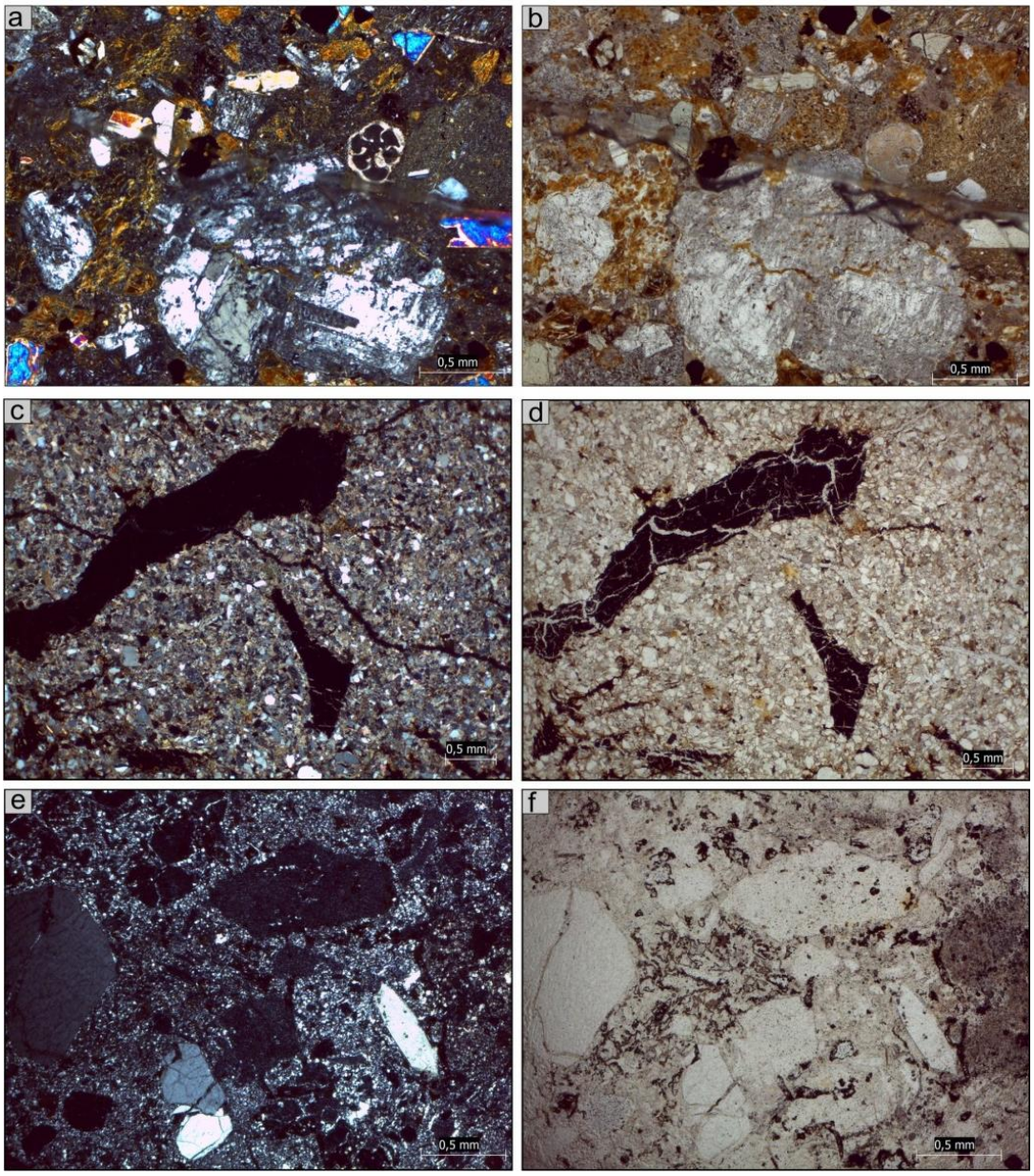

Figure 2. 7 : Photomicrographs of volcaniclastic rocks from İshaklı Formation. a-b) Thin section of lithic tuff containing plagioclase and amphibole minerals, volcanic rock fragment, and pelagic fossil (XPL, PPL). c-d) coal-containing volcanic sandstone in a turbidit

Planktic foraminifera fossils were found in the thin-sections from sandstones forming the turbiditic sequence (Figure 2.8). Planktic foraminifera (Sample no: 286a) are *Globotruncanita cf. elevata* (Brotzen), *Globotruncana cf. arca* (Cushman), and *Globigerinelloides sp.* and gives the age of Campanian-Maastrichtian; (possibly Campanian?) (determined by paleontologist Prof. Dr. Ercan Özcan).

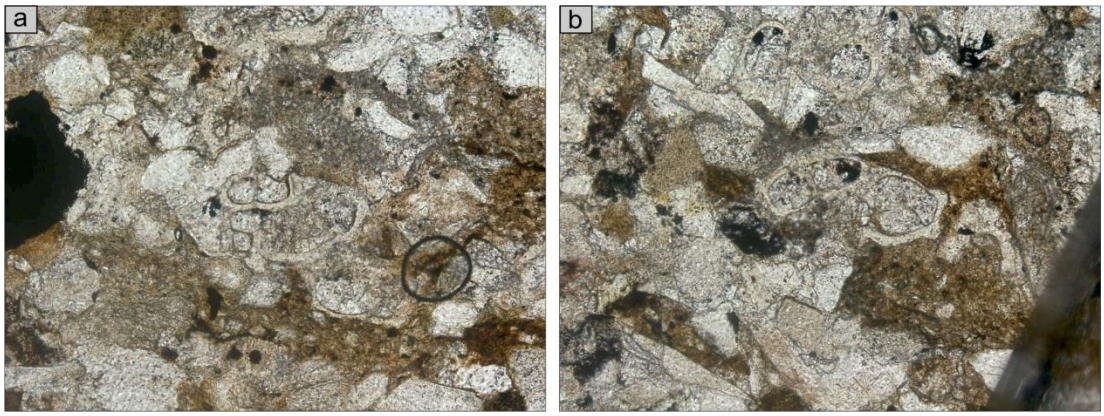

Figure 2.8 : Photomicrographs of sandstones from the İshaklı Formation.a) sandstone containing Globotruncanita cf. elevata (Brotzen), b) sandstone containing Globotruncana cf. arca (Cushman) (Sample location: X:4559300 Y:6889455).

LA-ICP-MS U-Pb zircon dating was performed on 23 zircon grains collected from a tuff level of the İshaklı Formation (Table 1). Zircons are euhedral and show oscillatory zoning that is typical for magmatic zircons. The results are discordant with different degrees. The Discordia age calculated is 75.45±1.38 Ma (Campanian) that was interpreted as crystallization age of the zircons and the age of the İshaklı Formation (Figure 2.9).

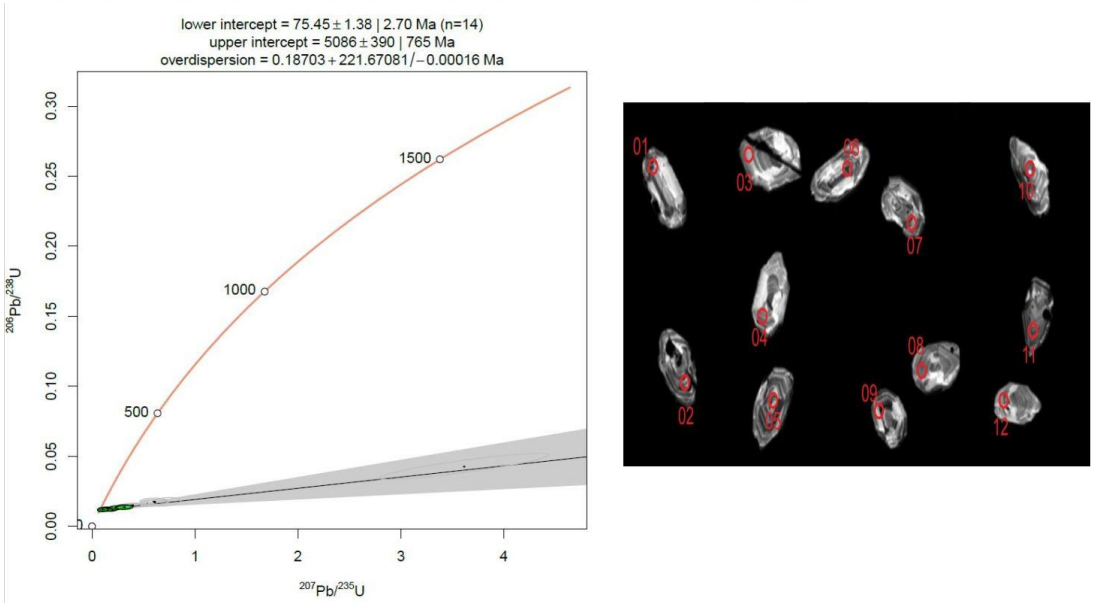

Figure 2.9 : a) Zircon U-Pb discordia diagrams from the tuff level (Sample no:266) of İshaklı Formation. b) Cathodoluminescence images of dated zircons from the tuff level of İshaklı Formation (Sample location: X:4558598 Y:6885736).

Table 1: LA-ICP-MS U-Pb isotopic data for zircons from the tuff level in the İshaklı Formation

Sample:266

Spot	U ppm	Pb ppm	Th ppm	Pb^{207}/U^{235}	±2σ	Pb^{206}/U^{238}	±2σ	RHO	U^{238}/Pb^{206}	±2σ	Pb^{207}/Pb^{206}	±2σ	Age Pb^{206}/U^{238}	±2σ
266_1	369,8	40,7	237	0,561	0,054	0,01592	0,00059	0,39	62,81407	2,327908	0,244	0,016	101,8	3,7
266_2	302	48,8	247	0,78	0,13	0,0176	0,0012	0,41	56,81818	3,873967	0,298	0,027	112,6	7,6
266_3	177,7	130	85,1	4,05	0,47	0,0428	0,0038	0,77	23,36449	2,074417	0,613	0,027	269	23
266_4	105,1	5,5	48,1	0,374	0,054	0,01477	0,0007	0,33	67,70481	3,208759	0,184	0,026	94,5	4,4
266_5	194	4,69	121	0,098	0,015	0,01219	0,0004	0,21	82,03445	2,691861	0,0583	0,0092	78,1	2,5
266_6	279,9	35,8	173	0,632	0,074	0,01744	0,00074	0,36	57,33945	2,432981	0,253	0,024	111,4	4,7
266_7	247,1	43,8	228,9	0,611	0,091	0,0177	0,001	0,38	56,49718	3,191931	0,246	0,026	113,3	6,4
266_8	164,2	6,96	82,6	0,165	0,025	0,01265	0,00048	0,25	79,05138	2,999578	0,096	0,015	81	3
266_9	282,3	10,54	258,4	0,094	0,014	0,01198	0,00037	0,21	83,47245	2,578031	0,0575	0,0086	76,8	2,3
266_10	123	5,16	73,9	0,145	0,022	0,01202	0,00051	0,28	83,19468	3,529891	0,09	0,014	77	3,3
266_11	174,4	4,79	103,5	0,103	0,02	0,01222	0,0005	0,21	81,83306	3,348325	0,072	0,015	78,3	3,2
266_12	145,9	12,6	85,6	0,428	0,052	0,01505	0,00062	0,34	66,44518	2,737277	0,191	0,02	96,2	4
266_13	222	6,63	120,2	0,151	0,017	0,01264	0,00043	0,30	79,11392	2,691376	0,089	0,011	81	2,7
266_14	145,1	5,09	76,2	0,189	0,027	0,01191	0,0005	0,29	83,96306	3,524897	0,109	0,016	76,3	3,2
266_15	131,8	5,62	67,1	0,23	0,027	0,01314	0,00058	0,38	76,1035	3,359211	0,125	0,015	84,1	3,7
266_16	149,3	11,8	91,6	0,394	0,043	0,01481	0,00051	0,32	67,52194	2,325199	0,188	0,02	94,7	3,2
266_17	158,7	7,67	110,3	0,152	0,023	0,01194	0,00047	0,26	83,75209	3,296774	0,091	0,015	76,5	3
266_18	131	7,52	76,8	0,291	0,031	0,01387	0,00058	0,39	72,09805	3,014915	0,158	0,017	88,7	3,7
266_19	128,4	7	70,6	0,308	0,032	0,01355	0,00063	0,45	73,80074	3,431326	0,17	0,018	86,7	4
266_20	135,8	16,36	71,8	0,613	0,05	0,017	0,00068	0,49	58,82353	2,352941	0,261	0,022	108,6	4,3
266_21	200,4	6,22	125,1	0,11	0,017	0,01241	0,00041	0,21	80,58018	2,662198	0,068	0,01	79,5	2,6
266_22	210	5,69	120	0,113	0,014	0,01176	0,00042	0,29	85,03401	3,036929	0,0734	0,0091	75,3	2,7
266_23	157	3,38	82,2	0,088	0,02	0,01191	0,00062	0,23	83,96306	4,370873	0,063	0,013	76,3	4

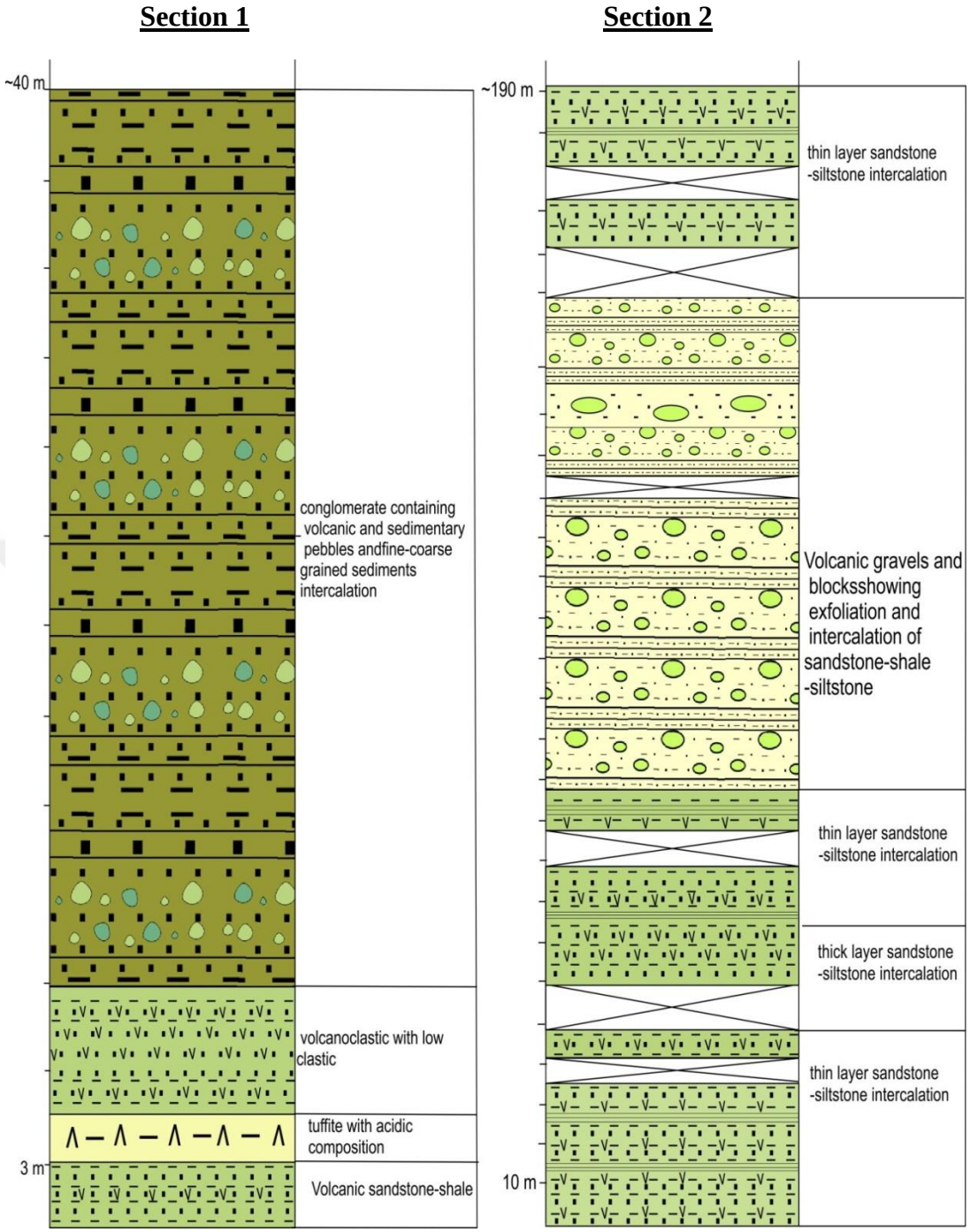

Figure 2. 10 : Measured stratigraphic section from İshaklı Formation. Its location is given as Section 1 and Section 2 on the geological map.

Lithostratigraphic features of the İshaklı Formation clearly indicate a fore-arc turbiditic origin for this unit. The İshaklı Formation is conformably and gradually overlain by the Riva Formation. Towards the upper part of the sequence, volcanic material increase and passes up to the Riva Formation which is characterized by basic and andesitetic lava flows.

2.4 Riva Formation

The Riva Formation consists of agglomerate, volcanic sandstone, tuff and andesitic-basaltic lavas. While the formation named as Cambu formation by Şahintürk and Özçelik (1983), Keskin et al. (2003) called it as the Garipçe Formation. The Riva Formation is well observed along the Black Sea coast, on both sides of the Bosphorus. It covers approximately an area of 21 km long to 7 km wide in the study area.

One of the detailed stratigraphic section is measured in the Riva Formation to understand depositional features of the succession. According to the stratigraphic section measured from the Riva Formation (Figure 2.21), the base of the unit starts with volca- noclastic rocks (Figure 2.11a and Figure 2.11d) and passed upward to highly altered and massive lavas (Figure 2.14b, c). The massive andesitic lavas are stratigraphically overlain by the debris flow deposits (Figure 2.11b, c). Volcanoclastic rocks include biotite and feldspar grains, fractures of clastic and volcanik rock derived from the base of the Riva Formation. The size of volcanic and clastic blocks in the debris flows increases from bottom to top (Figure 2.11b). The debris flow deposits are stratigraphically overlain by the the massive andesitic lavas (Figure 2.11d).

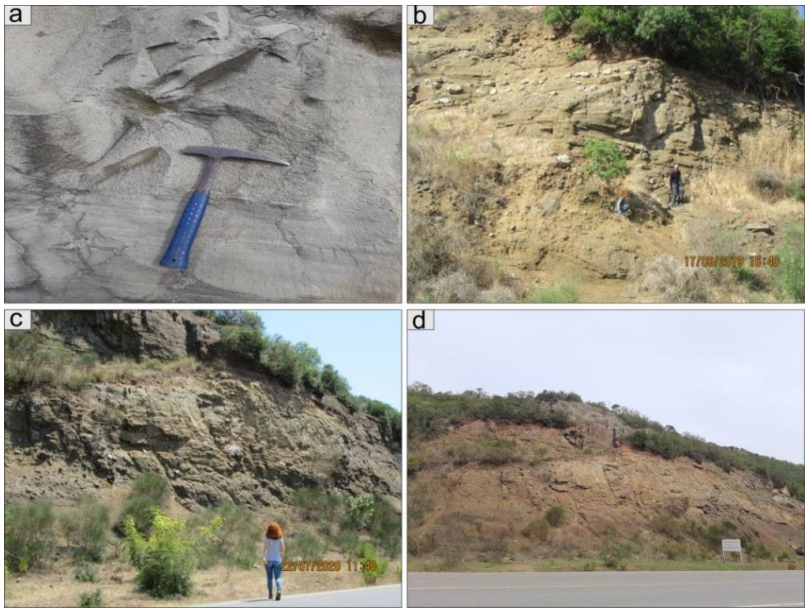

Figure 2. 11 : Field photographs of Riva formation a) The lithic tuff level within the volcaniclastic sequence, b-c) Debris flow observed within the Riva Formation, d) andesitic lavas covering debris flow deposits.

Agglomerates crop out to the north of the study area and are covered by andesitic lavas **(**Figure 2.12d). The agglomerates are cut by andesitic dykes (Figure2.12a and Figure 2.15a) Andesitic rocks are often highly altered and filled with secondary minerals such as chalcedony and calcite along the fractures and fissures (Figure 2.13c). Blocks and pebbles of agglomerates are composed of andesitic, vitrophyre, and basaltic rock fragments (Figure 2.12c). The grains are variable in size (5 cm - 30 cm), moderately sorted and poorly rounded. Agglomerates are matrix supported and the matrix surrounding the grains is stiff and very durable (Figure 2.12c, d). The lavas are black and dark gray and have fine-grained and porphyritic-aphanitic texture.

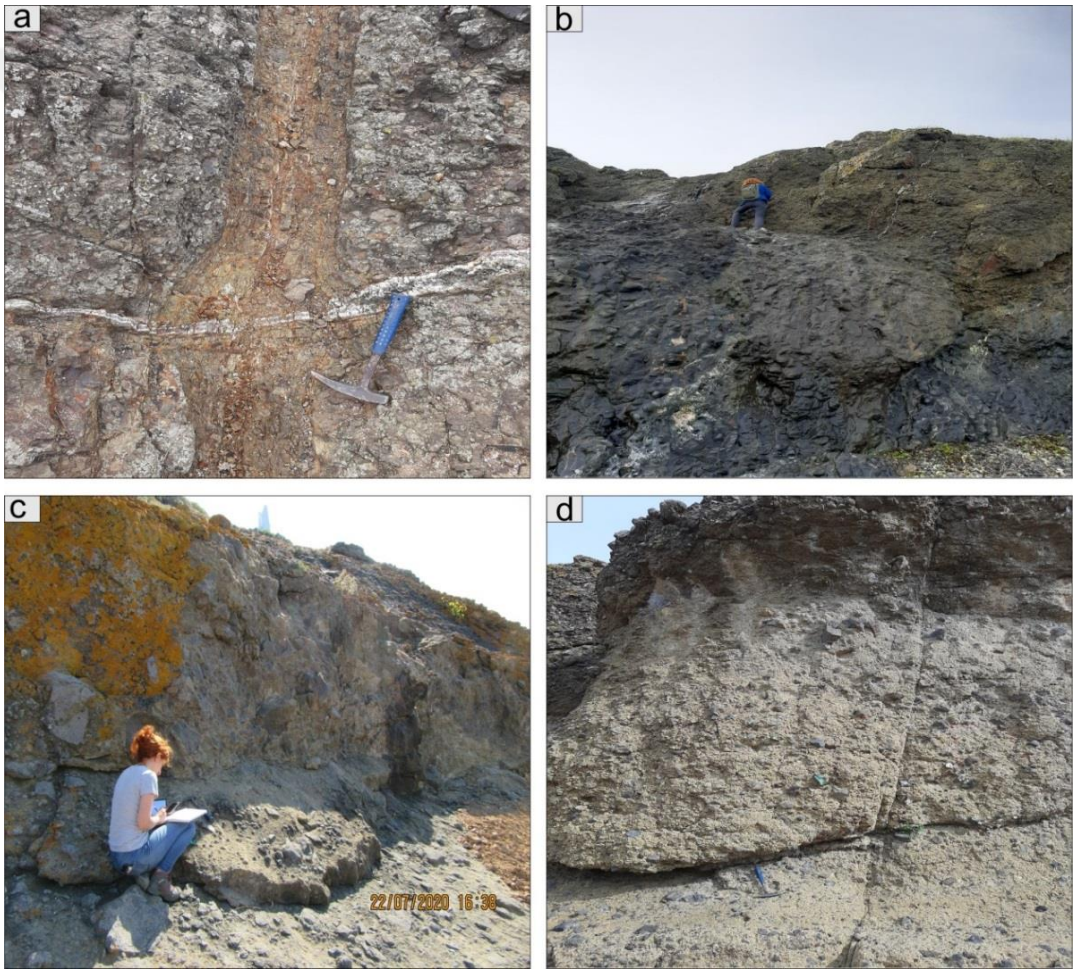

Figure 2. 12 : Field photographs of İshaklı formation a-b) andesitic dyke cutting the agglomerates east of Elmas Burnu, Riva. c-d) agglomerates composed of volcanic pebble, Riva beach.

As a result of K-Ar dating based on basaltic andesites equivalent to the Riva Formation in İğneada, the age of the Riva Formation was determined as Campanian by Ercan et al. (1998) (Gedik et al., 2005)

Figure 2.13 : Field photographs of İshaklı formation. a) andesitic lavas containing volcanic glass, b) andesitic lava with pronounced flow directions, c) chalcedony minerals that have filled the fissure of volcanic rocks, d) volcaniclastics containing fragments of volcanic rock overlying agglomerates.

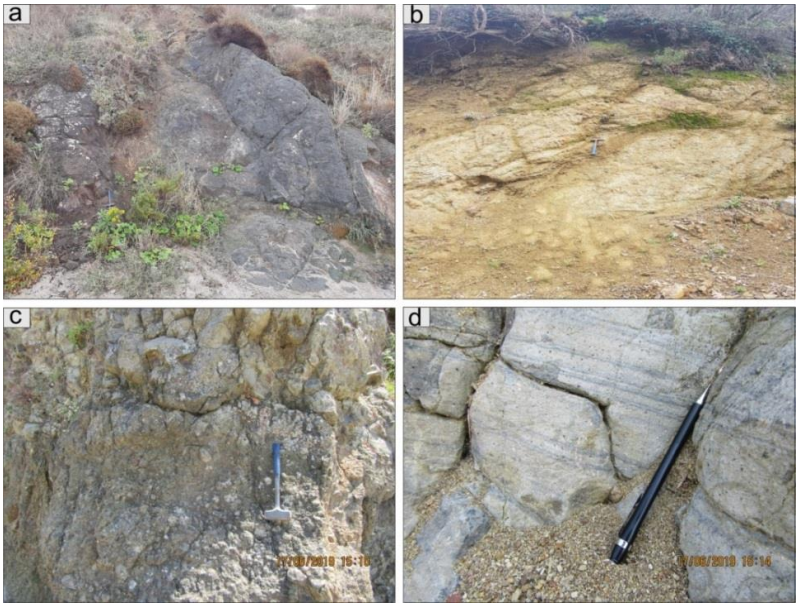

Figure 2.14 : Field photographs of Riva Formation a) andesitic dyke cutting volcaniclastics, b-c) altered andesitic lavas, d) Fine-grained volcaniclastics with lamination.

Basaltic and andesitic lava samples exhibit porphyritic texture (Figure 2.15). Phenocrystals in the rock are composed of plagioclase, amphibole, and pyroxene minerals (Figure 2.16a,b and Figure 2.17c,d). They have volcanic glass or fine-grained groundmass. Plagioclase minerals have polysynthetic twinning, and sieve textures (Figure 2.15a, b and Figure 2.18c,d) that reflect the instability conditions in the magma chamber. Although the sieve texture is interpreted as a magma mixing by some researchers, it can be formed as a result of rapid decompression (Nelson and Montana, 1992). Hornblende minerals are euhedral and have two excellent cleavages. They have green pleochroism in plane polarised light (Figure 2.15c, d). Basalts contain plagioclase, pyroxene and amphibole minerals and have glassy texture, while the matrix of andesites is represented by plagioclase microlites.

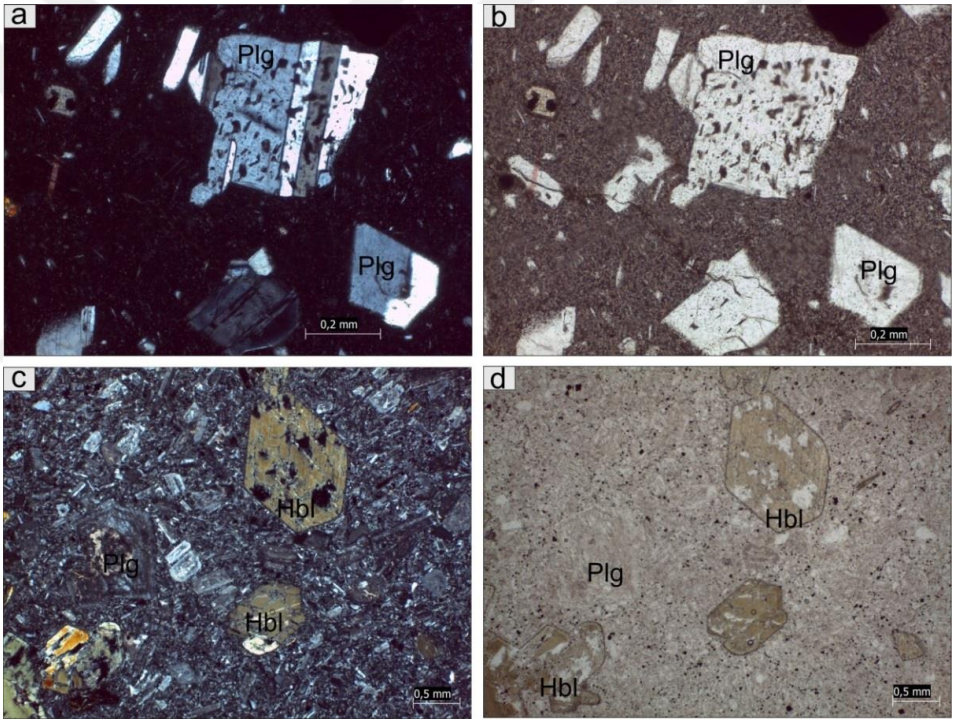

Figure 2.15 : Thin section images of rocks belonging to the Riva formation. a-b) plagioclase (plg) phenocryst which exhibit sieve texture of basalt rock with volcanic glass groundmass (XPL,PLL). c-d) Hornblende phenocryst of andesitic rock with fine-grained plagioclase groundmass (XPL, PPL).

Pyroxenes are generally augites, but orthopyroxene minerals are also observed in the thin sections (Figure 2.16a, b). They have brownish pleochroism in plane polarised light. Some of the lava samples have vesicular and amygdaloidal textures (Figure 2.16c, d). Amygdales are filled with secondary minerals such as zeolite.

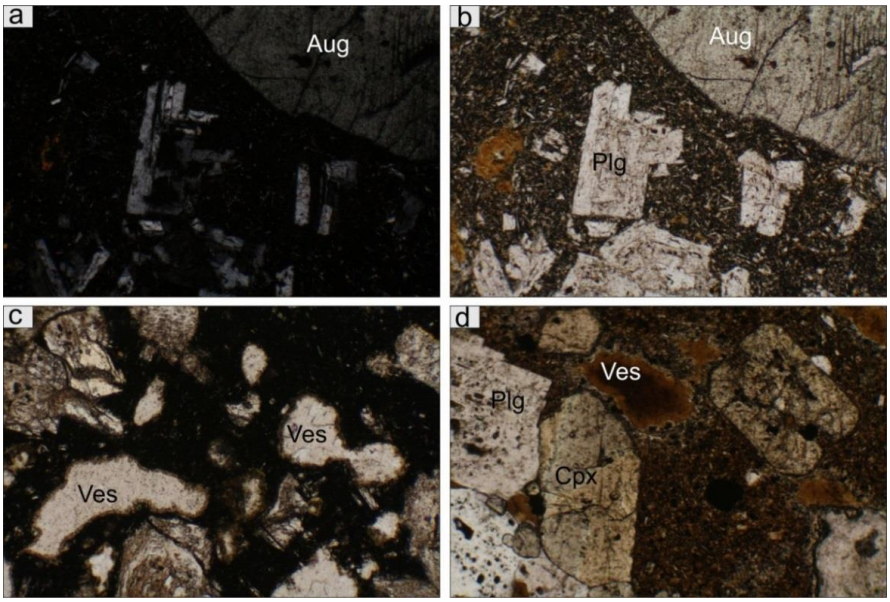

Figure 2. 16 : Thin section images of volcanic rocks of the Riva formation. a-b) plagioclase and augite phenocrysts with fine-grained plagioclase and pyroxene groundmass, porphyritic texture (XPL, PPL). c) basalt rock with vesicular texture (PPL). d) inclusion-containing plagioclase and clinopyroxene phenocrysts (PPL).

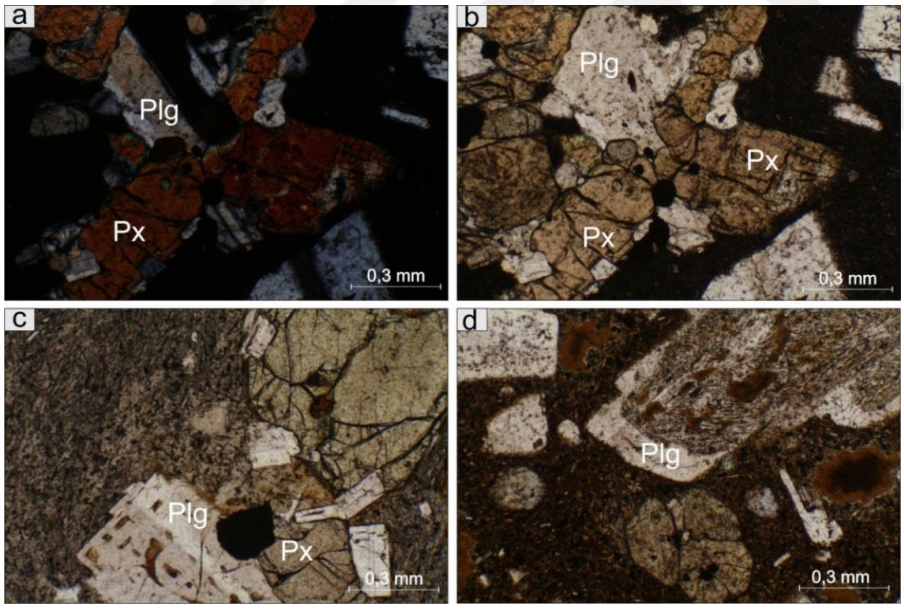

Figure 2. 17 : Thin section images of volcanic rocks of the Riva formation. a-b) pyroxene and plagioclase phenocrysts surrounded by the fine-grained groundmass (XPL, PPL). c) inclusion-containing plagioclase, pyroxene, and amphibole phenocrysts in a slightly oriented fine-grained matrix (PPL) d) plagioclase phenocryst displaying two different growth stages in amygdaloidal basalt (PPL).

In the Riva formation, tuffs are divided into two as lithic and crystalline tuffs. Lithic tuffs contain different types of volcanic material (Figure 2.18c,d). Clay formation is

observed in places in volcanic particles. Crystalline tuffs contain abundant plagioclase, hornblende, and opaque minerals that have partly oxidized (Figure 2.18a,b). Calcites were formed as secondary minerals. Some amphibole minerals are surrounded by volcanic glass (Figure 2.18b).

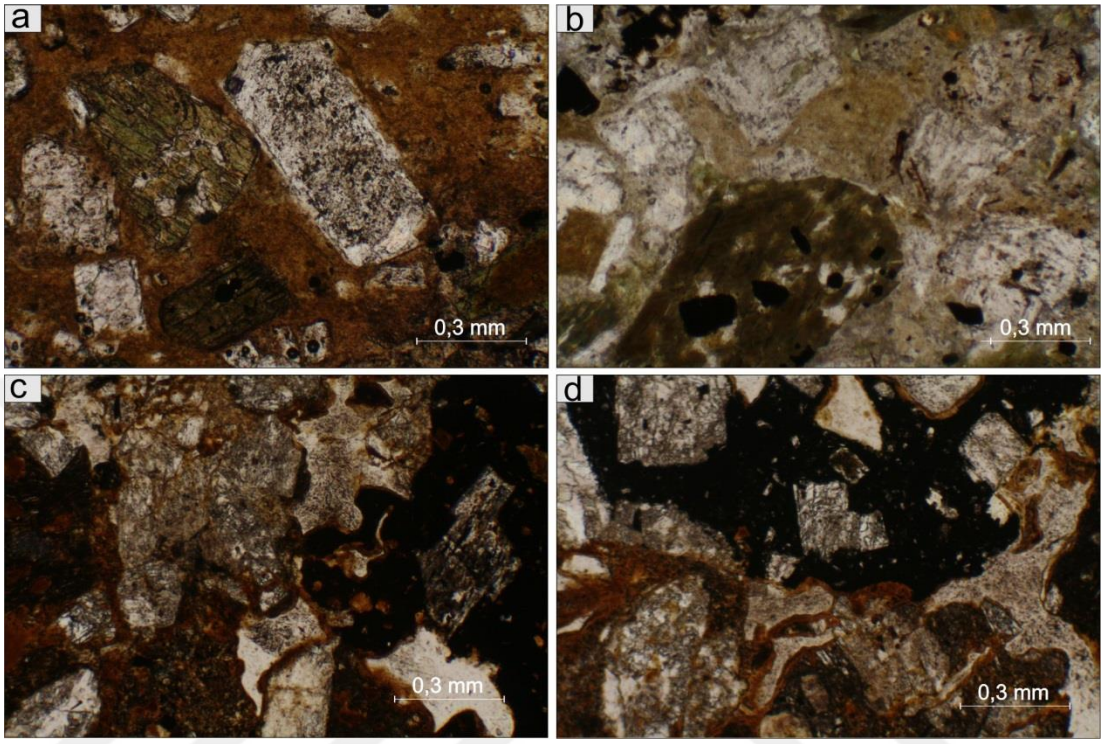

Figure 2. 18 : Thin section images of rocks belonging to the Riva formation. a) hornblende and plagioclase minerals surrounded by volcanic glass in crystalline tuff (PPL). b) opaque minerals and plagioclase minerals in crystalline tuff (PPL). c-d) lithic tuff with different types of volcanic material (PPL).

For the dating of the unit U-Pb zircon method was performed on two different tuff samples (the samples 12b and 221) in the Riva formation. The U-Pb dating was conducted on 22 zircon grains from the sample 12b and 18 zircons grain from the sample 221 (Table 2 and Table 3). According to measurements and relavent calculations, the age of the Riva formation is obtained as 78.46±1.17-76.29±2.48 Ma (Campanian) (Figure 2.19 and Figure 2.20).

Table 2: : LA-ICP-MS U-Pb isotopic data for zircons from the tuff level in the Riva Formation.

Sample 221

Spot	U ppm	Pb ppm	Th ppm	Pb^{207}/U^{235}	±2σ	Pb^{206}/U^{238}	±2σ	RHO	U^{238}/Pb^{206}	±2σ	Pb^{207}/Pb^{206}	±2σ	Age Pb^{206}/U^{238}	±2σ
221_1	189	11,7	234	0,159	0,021	0,01251	0,00046	0,28	79,93605	2,939295	0,099	0,013	80,1	2,9
221_2	92,5	6,22	53,4	0,329	0,042	0,01353	0,00065	0,38	73,90983	3,550731	0,179	0,023	87	4,1
221_3	164,4	11,2	98,1	0,377	0,055	0,01297	0,00088	0,47	77,101	5,231217	0,219	0,03	83	5,6
221_4	115,9	7,43	88,1	0,256	0,042	0,01214	0,0006	0,30	82,37232	4,07112	0,166	0,028	77,8	3,8
221_5	122,4	4,22	76,2	0,177	0,027	0,01132	0,00054	0,31	88,33922	4,214062	0,121	0,019	72,5	3,4
221_6	100,7	15	62,8	0,62	0,045	0,01724	0,00067	0,54	58,00464	2,254241	0,258	0,021	110,1	4,2
221_7	129,2	13,7	103,7	0,549	0,091	0,0157	0,001	0,38	63,69427	4,05696	0,239	0,035	100,3	6,6
221_8	114,9	4,25	63,7	0,161	0,026	0,01297	0,00058	0,28	77,101	3,447847	0,091	0,016	83,1	3,7
221_9	159,8	8,2	122,5	0,164	0,021	0,01228	0,00052	0,33	81,43322	3,448312	0,101	0,014	78,7	3,3
221_10	85	3,73	51,4	0,195	0,036	0,01235	0,00067	0,29	80,97166	4,392795	0,123	0,024	79,1	4,2
221_11	168,9	12,1	121,8	0,319	0,059	0,01361	0,00067	0,27	73,47539	3,617084	0,167	0,025	87,1	4,2
221_12	89,7	5,27	47,43	0,249	0,036	0,01222	0,00067	0,38	81,83306	4,486755	0,157	0,024	78,2	4,3
221_13	120,1	4,79	80,8	0,211	0,027	0,01238	0,0005	0,32	80,77544	3,262336	0,132	0,019	79,3	3,2
221_14	162	11,2	94,6	0,373	0,083	0,0127	0,0012	0,42	78,74016	7,440015	0,226	0,054	81,4	7,6
221_15	130,5	6,89	83,8	0,289	0,036	0,01336	0,00067	0,40	74,8503	3,75372	0,174	0,023	85,5	4,3
221_16	100	12,3	57,4	0,443	0,063	0,01635	0,00083	0,36	61,16208	3,104864	0,198	0,027	104,5	5,3
221_17	106,6	7,27	60	0,301	0,046	0,01377	0,00067	0,32	72,62164	3,533515	0,164	0,025	88,1	4,2
221_18	114,4	6,9	100,8	0,184	0,024	0,01305	0,00051	0,30	76,62835	2,994671	0,107	0,015	83,6	3,3
221_19	76,5	2,51	36,7	0,159	0,041	0,01302	0,00074	0,22	76,80492	4,365256	0,086	0,023	83,3	4,7
221_20	93,3	3,11	51,79	0,155	0,032	0,01201	0,00067	0,27	83,26395	4,645033	0,098	0,021	76,9	4,3
221_21	151,9	7,46	135	0,207	0,026	0,01232	0,00046	0,30	81,16883	3,030654	0,137	0,019	78,9	2,9
221_22	130,9	6,26	99,9	0,188	0,031	0,01351	0,00058	0,26	74,01925	3,177732	0,102	0,018	86,5	3,7

Table 3: LA-ICP-MS U-Pb isotopic data for zircons from the tuff level in the Riva Formation

Sample:12B

Spot	U ppm	Pb ppm	Th ppm	Pb^{207}/U^{235}	±2σ	Pb^{206}/U^{238}	±2σ	RHO	U^{238}/Pb^{206}	±2σ	Pb^{207}/Pb^{206}	±2σ	Age Pb^{206}/U^{238}	±2σ
12B_1	100	2,56	44,7	0,127	0,02	0,01146	0,00047	0,26	87,26003	3,578727	0,089	0,015	73,4	3
12B_2	119,8	2,99	65	0,107	0,021	0,01217	0,00047	0,20	82,16927	3,173341	0,067	0,013	78	3
12B_3	270	7,2	175,9	0,083	0,011	0,01211	0,00031	0,19	82,57638	2,113846	0,0513	0,0067	77,6	2
12B_4	132,3	272	71,5	13,8	2,8	0,124	0,02	0,79	8,064516	1,300728	0,731	0,038	730	100
12B_5	173,7	4,31	74,6	0,149	0,018	0,01303	0,00037	0,24	76,74597	2,179279	0,085	0,011	83,5	2,3
12B_6	106,6	2,61	46,2	0,095	0,02	0,01302	0,00049	0,18	76,80492	2,890508	0,058	0,012	83,3	3,1
12B_7	138,1	3,71	85	0,132	0,018	0,01274	0,00039	0,22	78,49294	2,402845	0,073	0,01	81,6	2,5
12B_8	111,3	6,49	80,7	0,27	0,028	0,01465	0,00053	0,35	68,25939	2,469452	0,142	0,015	93,7	3,4
12B_9	313	15,74	298,3	0,132	0,013	0,01293	0,00027	0,21	77,33952	1,614978	0,0749	0,0073	82,8	1,7
12B_10	146,3	9,11	185	0,091	0,017	0,01243	0,00065	0,28	80,45052	4,206986	0,061	0,013	79,6	4,1
12B_11	172	6,7	47,2	0,287	0,043	0,014	0,001	0,48	71,42857	5,102041	0,143	0,019	89,5	6,6
12B_12	59,5	2,05	50,4	0,144	0,041	0,01214	0,00062	0,18	82,37232	4,206824	0,102	0,029	77,8	4
12B_13	55,5	6,31	42,81	0,501	0,067	0,01485	0,00073	0,37	67,34007	3,31032	0,232	0,03	95	4,7
12B_14	119,6	30,2	160	0,696	0,05	0,0452	0,0011	0,34	22,12389	0,538413	0,1116	0,0076	285,1	6,6
12B_15	84,8	4,06	58,6	0,253	0,041	0,01352	0,00052	0,24	73,9645	2,844788	0,139	0,025	86,5	3,3
12B_16	200,2	34,2	232	0,371	0,022	0,04347	0,00079	0,31	23,00437	0,418069	0,0602	0,0036	274,3	4,9
12B_17	170,6	5,05	107,4	0,117	0,015	0,01289	0,00042	0,25	77,57952	2,527804	0,0671	0,0091	82,6	2,7
12B_18	85,3	3,08	47,3	0,164	0,025	0,01345	0,00058	0,28	74,34944	3,206147	0,094	0,015	86,1	3,7

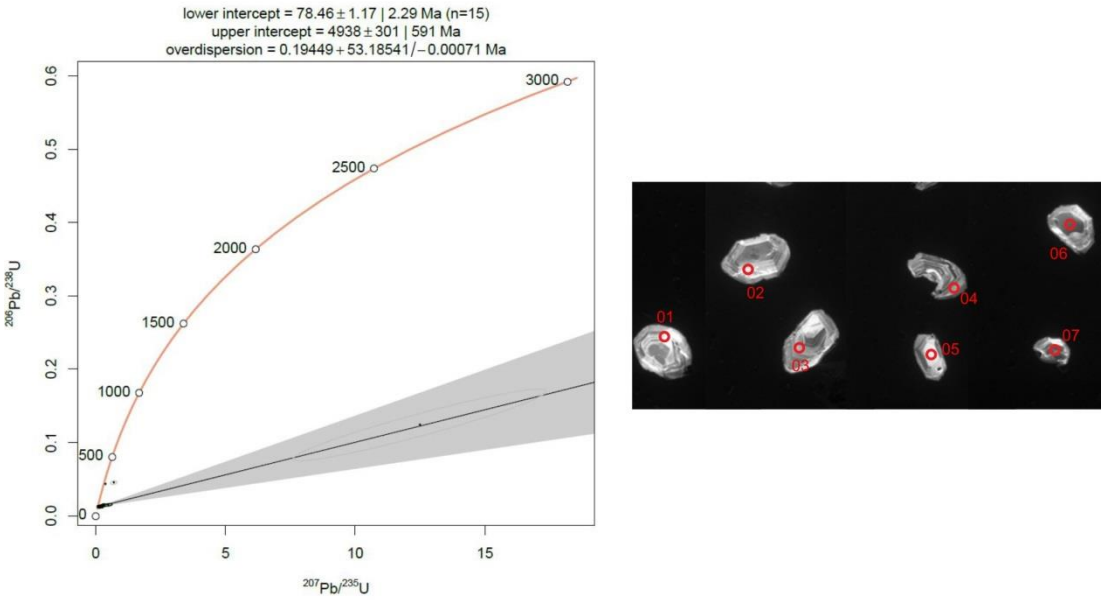

Figure 2. 19 : a) Zircon U-Pb discordia diagrams from the tuff level (sample 12b) of Riva Formation. b) Cathodoluminescence images of dated zircons from the tuff level of Riva Formation (Sample location: X:4567920 Y:6886767)

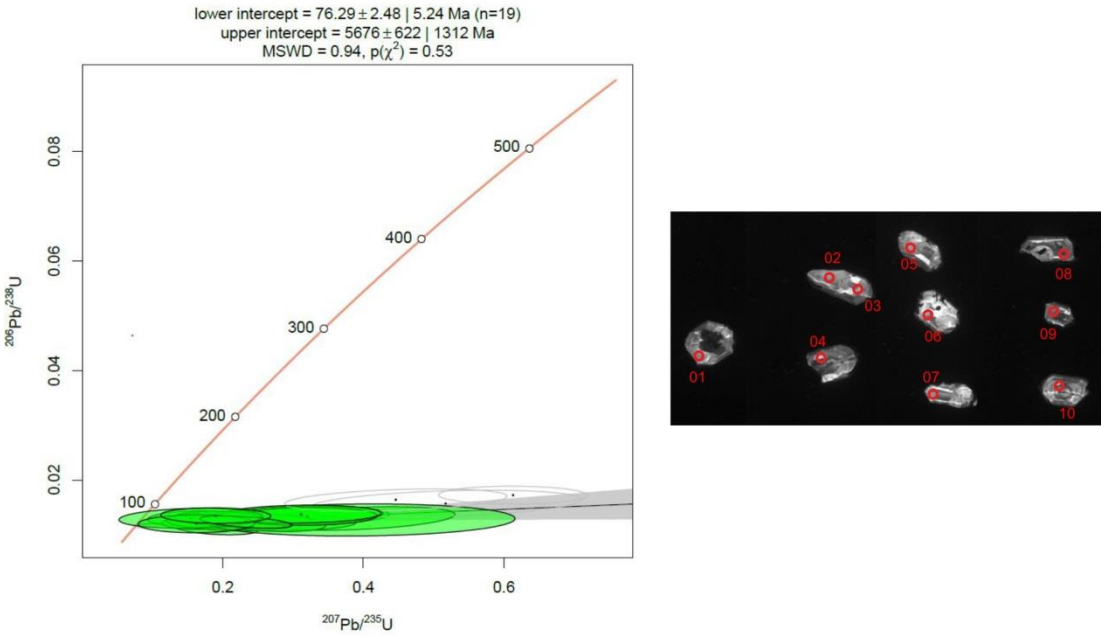

Figure 2. 20 : a) Zircon U-Pb discordia diagrams from the tuff level (sample 221) of Riva Formation. b) Cathodoluminescence images of dated zircons from the tuff level of Riva Formation (Sample location: X:4564886 Y:6897569).

Section 3

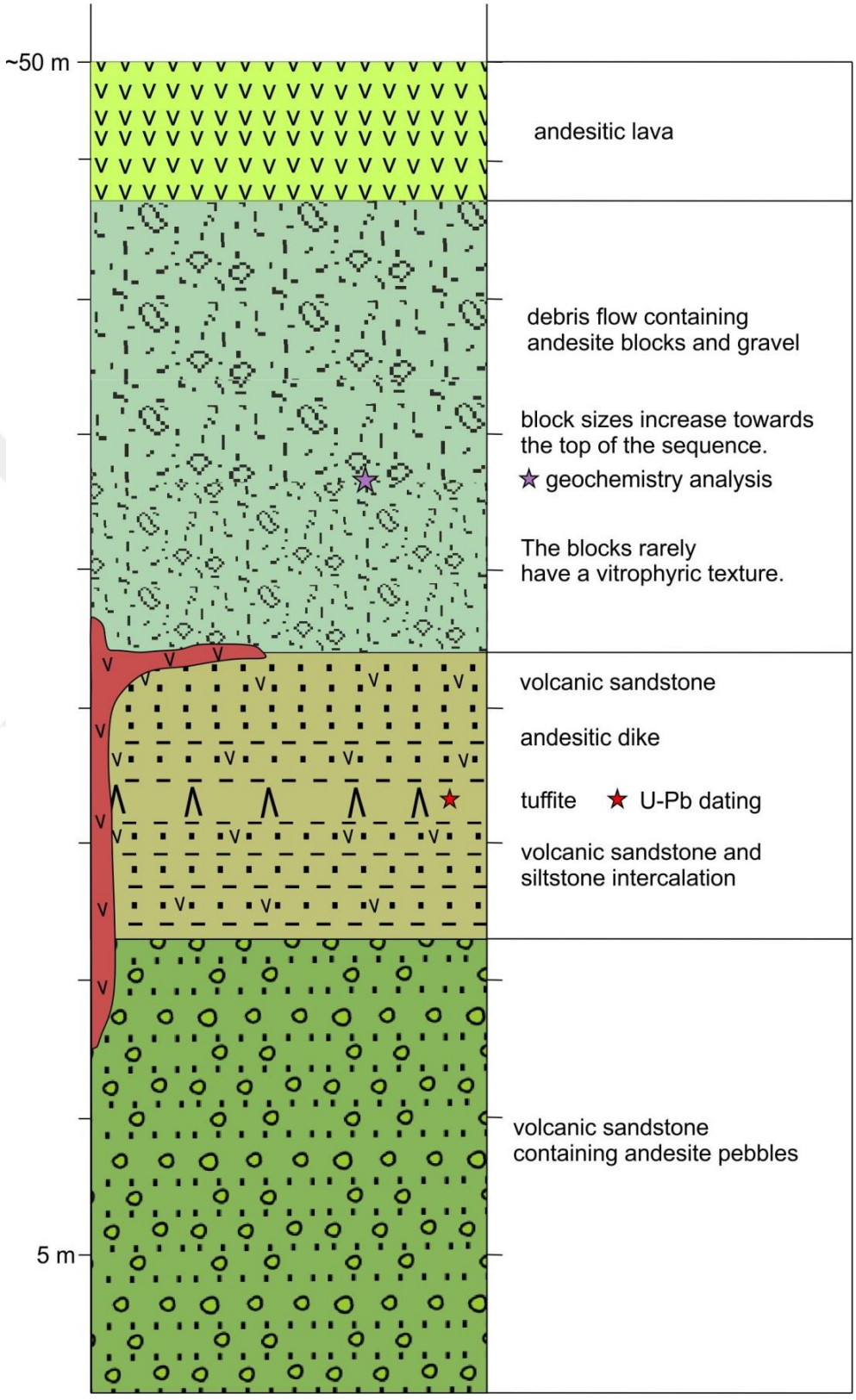

Figure 2. 21 : Detailed stratigraphic section measured through the Riva formation. Its location is given as Section 3 on the geological map.

2.5 Neogene Sediments

Neogene deposits are one of the most common units in the study area and crop out mostly in the top of the hills. They consist of unconsolidated gravel, sand, and silt representing the typical deposits of the terrestrial environment (Figure 2.22). With the termination of the volcanism and the uplift of the region, erosional flats were formed in the study area. Neogene sediments have been deposited in these erosional flats. Neogene sediments unconformably overlie the Riva and the İshaklı formations (Figure 23).

Neogene deposits offer economically important clay reserves (Yeniyol and Ercan., 1990). It has been suggested that these clays were formed as a result of the transport of detritic material and precipitation in the lake environment (Yeniyol and Ercan.; 1990). In the upper parts of the Neogene sequence, there is a very loose pebbly sandy unit reflecting a fluvial environment (Yeniyol and Ercan.; 1990).

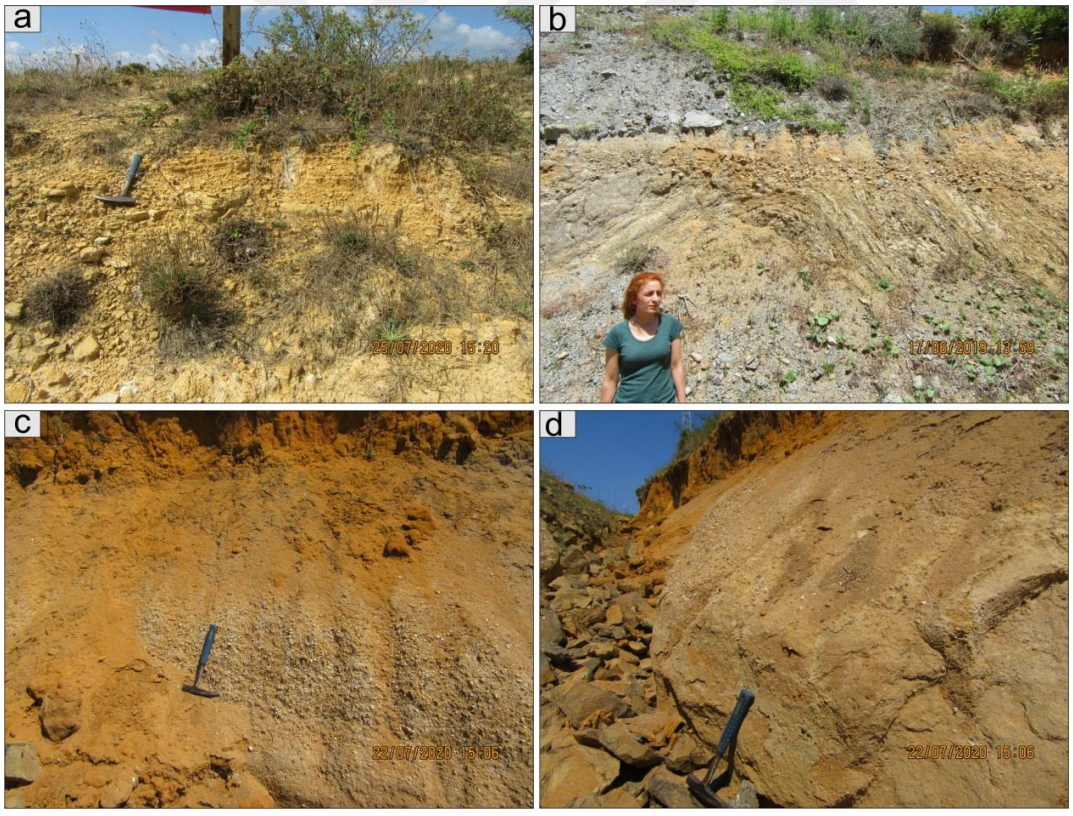

Figure 2. 22 : The field photograpy of Neogene sediments a) horizontally bedded sandstones. b) Neogene terrestrial sediments unconformably overlying the folded volcaniclastic sequence of the İshaklı formation. c-d) fluvial sediments composed of sand and gravel.

Figure 2. 23 : Neogene terrestrial sediments unconformably overlying columnar basalt. (west of the Riva Road, Locality 31)

3. GEOCHEMİSTRY

Whole-rock analyses were performed on 6 volcanic rock samples (C11a, C88, C13, C31, C91, C125) from the Riva Formation. Major oxides, trace elements, and rare earth elements composition of rocks were used to interpret the chemical properties and geodynamic environment of the volcanism. The rocks have varying degrees of alteration and volatile compostion. Volatile amount in the rock are given as 'Loss On Ignition' (LOI) value as percentage (%) in the analysis result (Table 4). Since the amount of LOI value of rocks varies, the main oxides are normalized to the LOI-free basis to enable comparison between analyzes. Volcanic rocks of the Riva Formation are divided into two as agglomerates and lavas. SiO_2 values of lavas range of between 55.00% and 56.81%, Al_2O_3 values between 17.42% and 18.17%, CaO values between 6.41% and 8.02%, K_2O values between 0.56% and 1.35%, Fe_2O_3 values between 7.23 % and 8.76%. SiO_2 values of agglomerates range of between 49.33 % and 64.48%, Al_2O_3 values between 15.09% and 16.87%, CaO values between 5.16% and 9.73%, K_2O values between 0.82% and 1.48%, Fe_2O_3 values between 5.15 % and 10.14%. The magnesium numbers (# Mg) of the rocks vary between 51.5%-32.6%. Considering that the Mg numbers of the melts coming from the primitive mantle vary between 65-75%, it is understood that the Riva Formation's volcanic rocks are highly differentiated.

3.1 Chemical nomenclature

In the classification of the volcanic rocks, TAS diagram proposed by Le Bas (1986), total alkali versus silica diagram, and Nb / Y-Zr / TiO_2 diagram proposed by Winchester and Floyd (1977) were used. According to the TAS diagram, C31 and C91 lava samples of the volcanic rocks of the Riva Formation fall into the basaltic andesite area, whereas the sample C125 fall into the andesite area. Agglomerates within the same unit present a more variable chemical composition compared to lava samples. As can be seen in Figure 3.1, the agglomerate samples C11a and C88 fall on the basalt-andesite boundary, and C13 falls in the dacite areas. In the chemical names of the volcanic rocks may not be correct because of the mobilisation of

elements such as K, Na in the samples as a result of alteration. For this reason, the Nb / Y-Zr / TiO_2 diagram, in which the the immobile Nb, Y, Zr and Ti elements were prefered, were also used to naming of the altered rock samples.

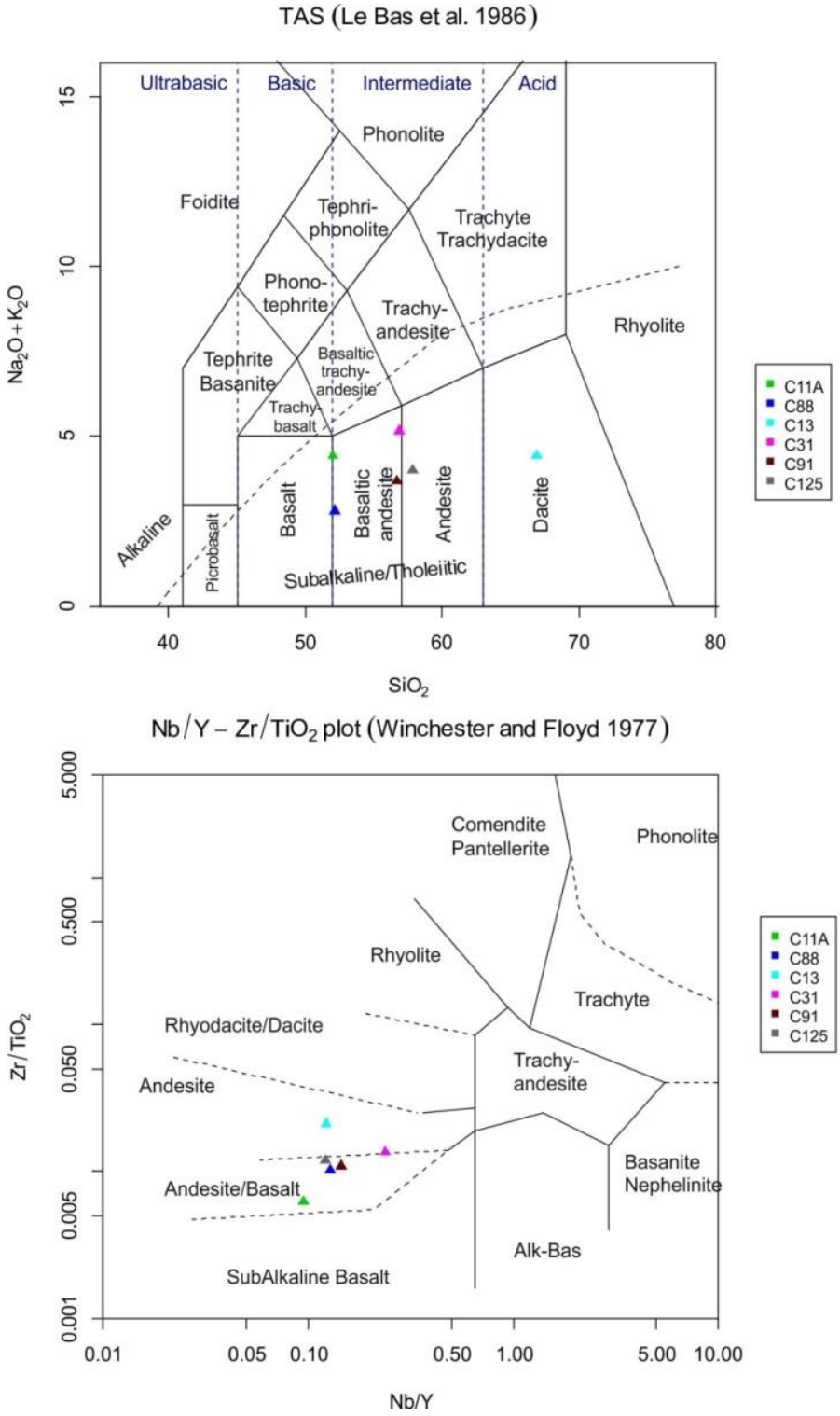

Figure 3. 1 : a) TAS (total alkali.silica) diagram of Le Bas et al. (1986) from Riva Formation b) SiO2-K2O diagram of Peccerillo and Taylor (1976) from Riva Formation.

According to the diagram, the C13 agglomerate sample in the Riva Formation falls into the andesite area, whereas the agglomerate samples C11a and C88 ploted in the basalt / andesite area. C91, C125 and C31 lava samples fall into the basalt / andesite area (Figure 3.1). Names of the samples derived from the chemical discrimination diagrams are also compatible with the petrographic observations examined on the thin sections of the samples. For the chemical classification of volcanic rocks, AFM diagrams constructed by alkali oxide ($Na_2O + K_2O$), iron oxide ($FeO + Fe_2O_3$), and magnesium oxide (MgO) amounts of the rocks were used (Irvin and Baragar, 1971). AFM diagrams are preferred to separate tholeiitic and calc-alkaline magma series in sub-alkaline magma series. The main oxides of volcanic rocks of the Riva Formation were plotted on the AFM diagram to reveal the magma chemistry. All of the volcanic rocks are located in the sub-alkaline area. In the K-SiO_2 diagram proposed by Peccerillo and Taylor (1976), the volcanic rocks belonging to the subalkali series are divided into low K (tholeiite), calc-alkali, high K calc-alkaline, and shoshonotic series.

The samples of the Riva Formation were plotted into this diagram and the agglomerate sample C13 falls into the tholeiitic area, while the agglomerate sample C88 falls into the calc-alkaline area and the agglomerate sample C11a falls into the high-K calc-alkaline area. Also, the C91 and C125 lava samples fall into the tholeiitic area and the C31 lava sample falls into the calc-alkaline area (Figure 3.2).

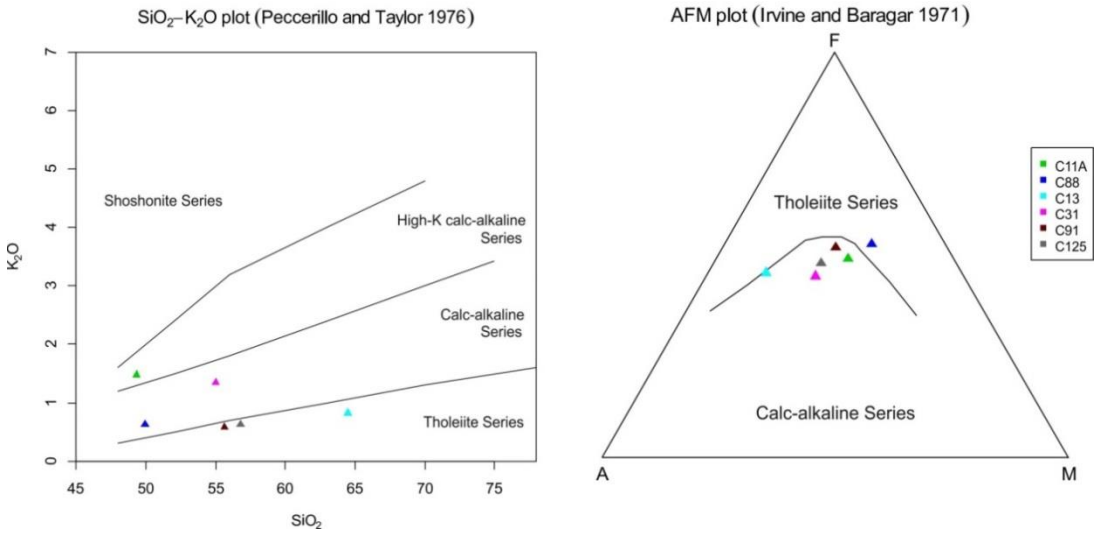

Figure 3.2 : a) Classification of volcanic rocks by the K2O-SiO2 diagram Peccerillo and Taylor (1976). b) Classification of volcanic rocks by the AFM diagrams (Irvin and Baragar, 1971).

Table 4 : Whole-rock geochemical analyses results of volcanic rocks from Riva Formation.

Sample No	C11A	C88	C13	C31	C91	C125
Rock Type	Basalt	Andesite/Basalt	Andesite	Andesite	Andesite/Basalt	Andesite/Basalt
SiO2	49,33	49,92	64,48	55,00	55,64	56,81
Al2O3	15,88	16,87	15,09	17,60	17,42	18,17
Fe2O3	10,14	10,06	5,15	7,83	8,76	7,23
MgO	5,28	5,42	1,26	3,69	3,69	3,12
CaO	8,84	9,73	5,16	6,41	8,02	8,01
Na2O	2,72	2,06	3,45	3,65	3,03	3,29
K2O	1,48	0,63	0,82	1,35	0,58	0,63
TiO2	0,79	0,70	0,64	0,84	0,75	0,64
P2O5	0,17	0,14	0,16	0,21	0,14	0,14
MnO	0,22	0,15	0,13	0,17	0,16	0,14
Cr2O3	0,006	0,004	<0.002	<0.002	0,003	0,002
LOI	4,9	4,1	3,5	3,1	1,6	1,6
Sum	99,75	99,77	99,91	99,83	99,83	99,84
Ba	408	185	336	269	196	206
Sc	33	30	15	18	27	22
Be	1	<1	<1	<1	2	<1
Co	31,5	31,3	8,4	18,0	23,1	19,0
Cs	1,4	0,2	5,7	1,5	1,6	3,1
Ga	11,8	13,9	12,1	15,4	15,2	14,8
Hf	1,4	2,2	4,0	3,0	2,4	2,1
Nb	1,8	2,4	3,7	5,0	3,3	2,7
Rb	22,1	6,2	59,0	31,9	20,0	32,8
Sn	<1	<1	1	<1	<1	<1
Sr	555,7	435,0	234,3	323,7	303,4	360,8
Ta	0,1	<0.1	0,3	0,3	0,2	0,2
Th	1,6	2,6	4,9	3,5	1,7	1,7
U	0,5	0,6	1,4	0,8	0,5	0,5
V	340	276	69	194	248	204
W	1,0	1,5	2,9	1,3	1,5	1,3
Zr	49,0	71,1	135,5	113,8	81,8	76,1
Y	18,9	18,8	30,3	21,0	22,8	22,2
La	9,3	11,0	15,1	16,4	10,7	11,4
Ce	18,6	23,2	32,5	33,6	23,5	23,4
Pr	2,55	3,22	4,01	4,18	3,20	3,06
Nd	11,9	14,1	18,3	17,2	13,8	13,8
Sm	2,84	3,37	4,07	3,88	3,49	3,26
Eu	0,95	1,00	1,02	1,22	1,02	0,95
Gd	3,42	3,63	4,91	3,97	4,00	3,60
Tb	0,53	0,58	0,82	0,62	0,64	0,61
Dy	3,36	3,58	5,10	3,86	4,22	3,86
Ho	0,75	0,76	1,20	0,81	0,91	0,83
Er	2,17	2,25	3,42	2,34	2,71	2,60
Tm	0,31	0,30	0,49	0,35	0,38	0,36
Yb	2,01	1,95	3,41	2,26	2,61	2,43
Lu	0,33	0,30	0,50	0,36	0,40	0,38
Mo	0,4	0,2	0,4	0,6	0,2	0,2
Cu	59,8	61,5	34,7	47,0	59,5	77,3
Pb	3,3	2,5	1,7	4,4	0,7	1,2
Zn	47	48	27	77	30	26
Ni	10,0	7,4	1,0	2,9	3,4	2,2
As	2,9	<0.5	1,4	1,9	1,7	0,7
Cd	<0.1	<0.1	<0.1	<0.1	<0.1	<0.1
Sb	<0.1	<0.1	<0.1	<0.1	<0.1	<0.1
Bi	<0.1	<0.1	<0.1	<0.1	<0.1	<0.1
Ag	<0.1	<0.1	<0.1	<0.1	<0.1	<0.1
Au	2,9	4,5	1,1	2,0	1,8	1,8
Hg	<0.01	<0.01	<0.01	<0.01	<0.01	<0.01
Tl	<0.1	<0.1	<0.1	<0.1	<0.1	<0.1
Se	<0.5	<0.5	<0.5	<0.5	<0.5	<0.5

3.2 Multiple element patterns of the volcanic rocks

3.2.1 Spider diagrams

The trace elements of the volcanic rocks of the Riva Formation were normalized according to the primitive mantle and plotted to the spider diagrams proposed by McDonough and Sun (1995). The trace element behaviors of the primary mantle differ as a result of the differentiation of the magma. When an igneous rock is formed, incompatible elements (Cs, K, Rb, Ba, Sr, Eu) are dissolved in fluids and enriched in melt, while the concentrations of compatible elements (Nb, Ta, Ti, Zr, Hf, Y) are controlled by the chemistry of the crystal / melt and source area (Pearce, 1983, Rollinson, 1993). For this reason, trace element groups exhibit different behaviors in different tectonic environments. The trace element concentrations of the volcanic rocks of the Riva Formation were normalized to concentrations of the reference primitive mantle values to obtained information about the tectonic environment where they formed.

The trace element concentrations of the lava and agglomerate samples were plotted to the spider diagram. All samples show Nb, Ta and Ti negative anomalies. Nb, Ta, and Ti trace elements are held by titanium minerals such as sphene, rutile, and ilmenite. During the differentiation of magma, Nb, Ta, and Ti elements are consumed in the remaining melt as a result of the separation of a titanium mineral from the magma and they show negative anomalies. In addition, negative Nb and Ta anomalies are characteristic for magmas of orogenic origin (Pearce, 1983, Rollinson, 1993).

While volcanic rocks are enriched by LILE elements, the depletion of HFSE elements and the relative height of the LILE / HFSE ratio is one of the indicators showing that the magma was formed in a subduction and/or an orogenic environment (Pearce and Peate, 1995). All of the volcanic rocks of the Riva Formation show positive Sr anomaly and enrichment in incompatible elements (Ba, Rb, Sr, Cs) (Figure 3.3). Considering all these features, volcanic rocks of the Riva Formation formed in an orogenic and/or subduction tectonic environment.

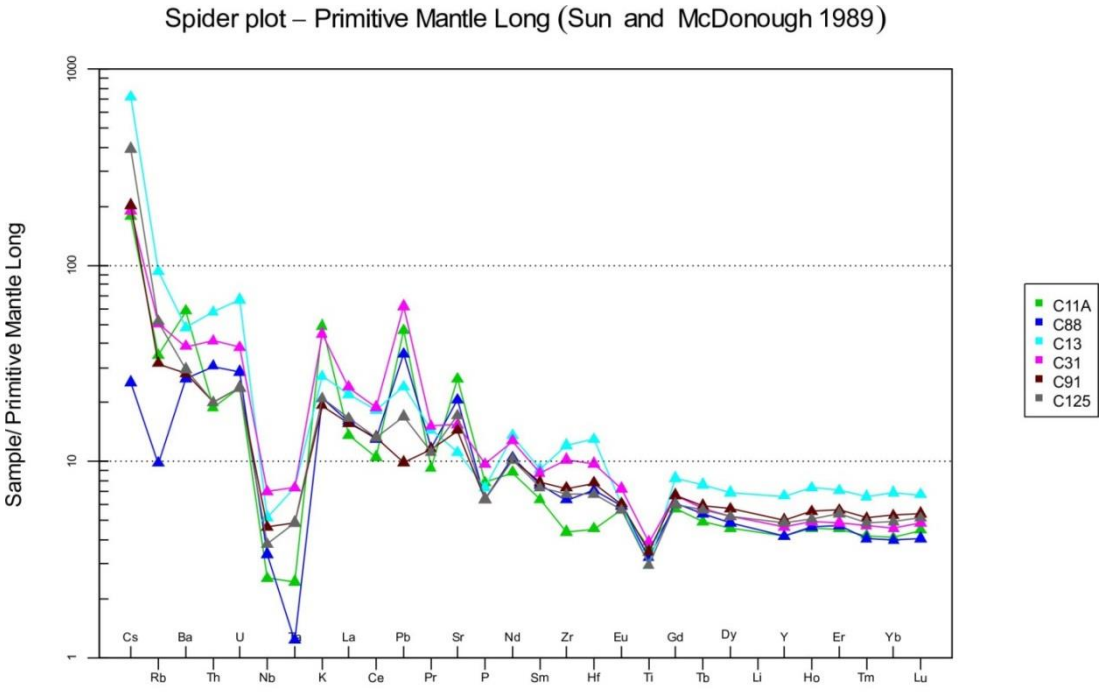

Figure 3. 3 : a) Primitive Mantle -normalized multi-element patterns of the lavas and agglomerates within the Riva Fm.

3.2.2 REE patterns of the Riva Formation's volcanic rocks

Rare-earth element (REE) contents measured from volcanic rocks were normalized according to the chondrites and rare earth element patterns were created. REE elements in volcanic rocks can be enriched or depleted according to the primitive composition as a result of fractional crystallization. Accordingly, it can be determined which mineral leaves the source area.

The chondrite-normalized REE pattern of the rocks displays slight negative Eu anomalies except for an agglomerate sample (C31) (Figure 3.4). Eu element is enriched in plagioclase minerals. As a result of crystallization of plagioclas during the differentiation of magma, Eu is consumed in the residual melt and exhibits negative anomaly (Green and Pearson, 1983). According to REE pattern, the rocks are enriched with light rare earth elements and slightly depleted by the heavy earth elements, which indicates that a mineral such as the garnet including heavy earth elements is not found in the source area.

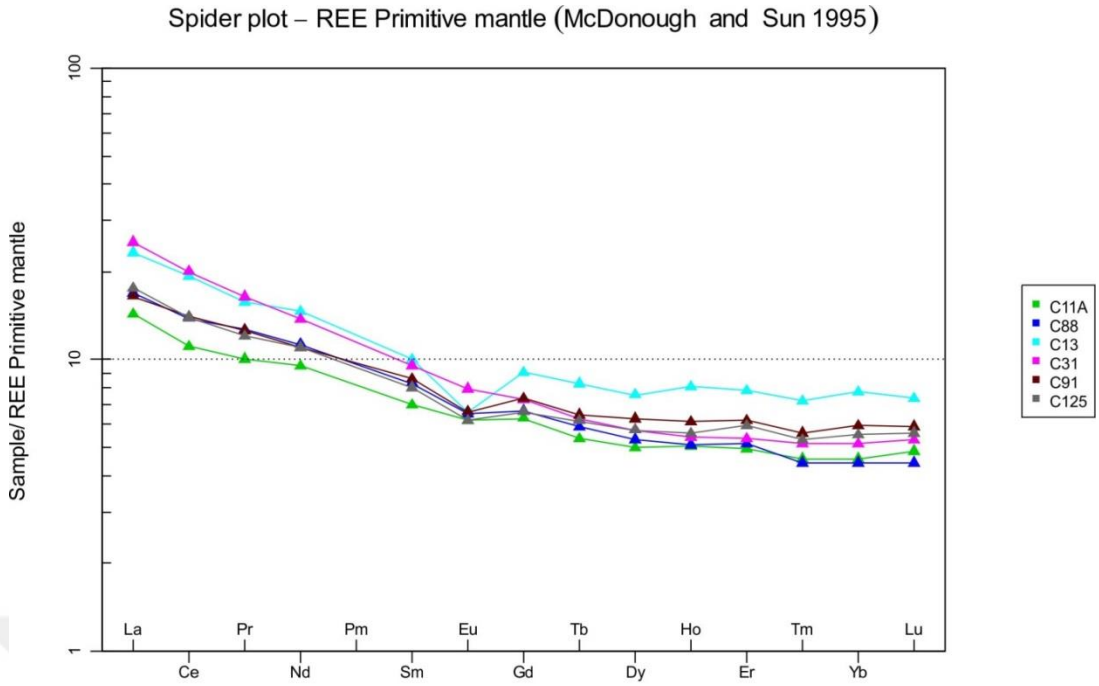

Figure 3. 4 : Chondrite-normalized REE patterns of the lav and agglomerates within the Riva Fm.

Harker diagrams were prepared based on SiO_2 and MgO values of the volcanic rock samples against their major or minor oxide concentrations. During the differentiation of magma, the values of MgO, CaO, TiO_2, and FeO decrease, while Al_2O_3, K2O, and Na_2O values increase against the increasing SiO_2 values. The increase of Na_2O and Eu values relative to SiO_2 values observed in Harker diagrams may indicate presence of plagioclase mineral especially enrichment in albite composition (Figure 3.5).

The decrease of MgO relative to SiO_2 indicates that a mineral containing Mg such as olivine, pyroxene, and amphibole leaves the the magma when differentiated. In the Harker diagrams, where generally MgO is compared to Ni element, as MgO decreases, the decrease of Ni element is one of the data supporting that olivine may be separated.

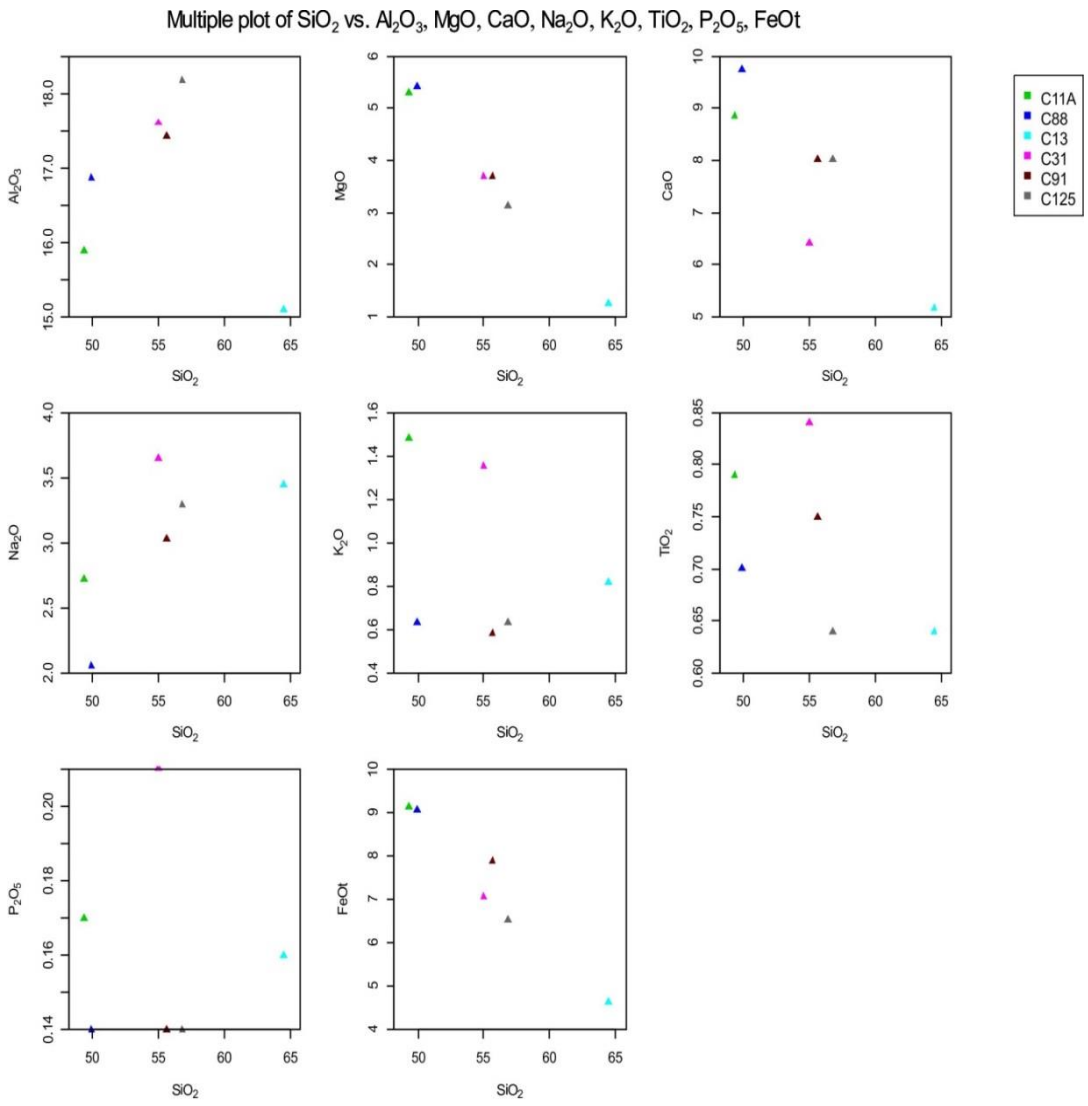

Figure 3. 5 : Harker diagrams for major elements of the lavas of Riva Formation.

While positive Sr anomaly is observed in the spider diagrams normalized relative to the primary mantle, in Harker diagrams Sr and CaO decrease in response to the increasing SiO_2 persantage during the differentiation of the magma. In the light of this information, it can be said that Sr element also separated from the melt during the differentiation of the magma related to a phase containing Ca such as plagioclase, amphibole, pyroxene crystallized. The volcanic rocks are enriched in incompatible elements such as Ce, Rb, Ba, and La. The Y element also shows enrichment in the Harker diagram (Figure 3.6). This can also be explained as the absence of garnet in the source area, which is one of the reservuars for Y.

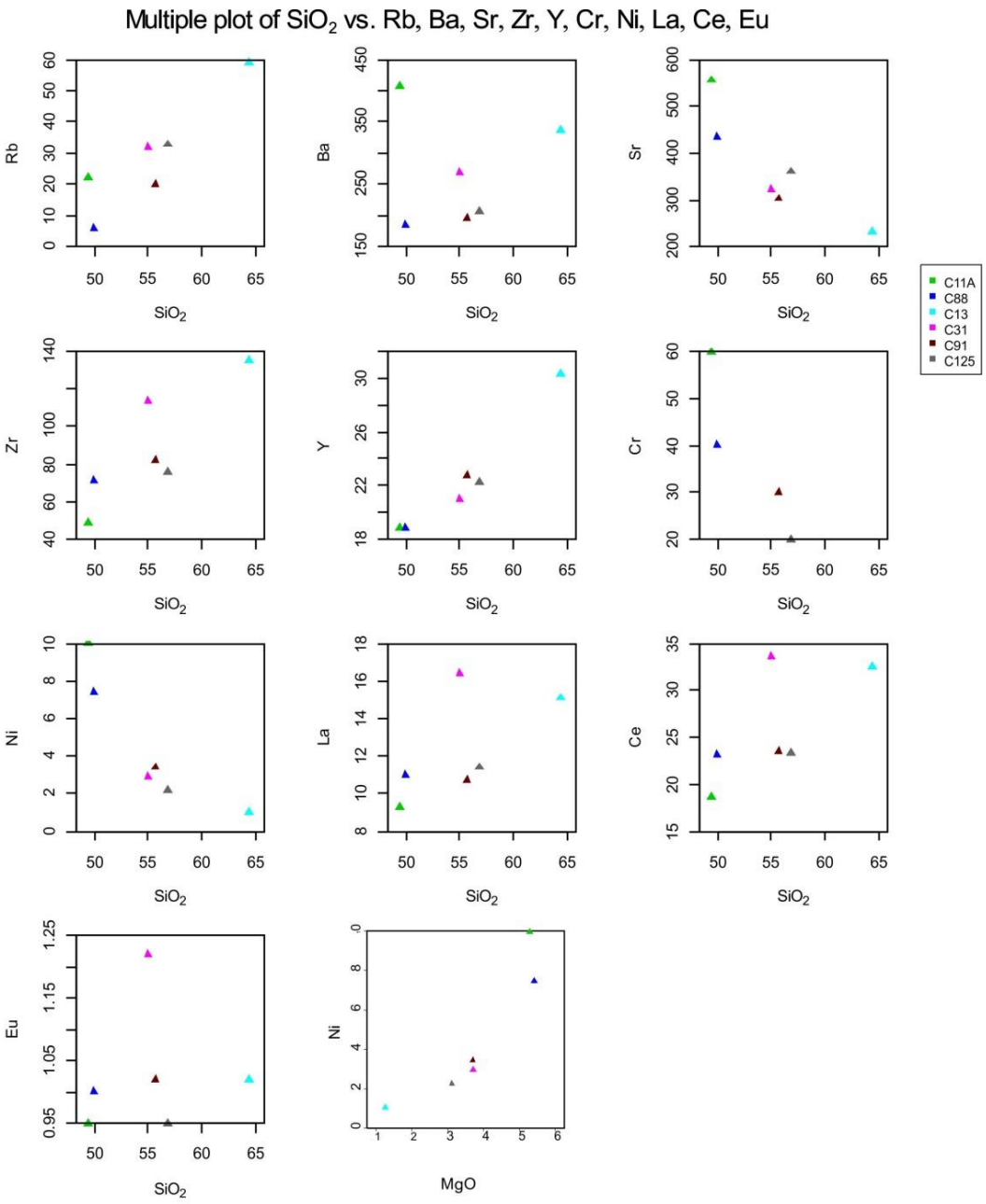

Figure 3. 6 : Harker diagrams for trace elements of the lavas of Riva Formation

3.3 General geochemical features of the Upper Cretaceous volcanic arc in the Pontides

The volcanic rocks of the Upper Cretaceous volcanic arc belt extend along the Black Sea coast in the Pontides, from Bulgaria in the west (Apuseni-Banat-Timok-Sredna-Gora belt) to Georgia in the east (Georgiev et al., 2009). In this section, to reveal the evolution of Upper Cretaceous arc volcanism, the temporal and spatial variation in magma character of different regions is examined and evaluated together with the volcanic rocks in the north of the Istanbul Zone (Figure.3.7).

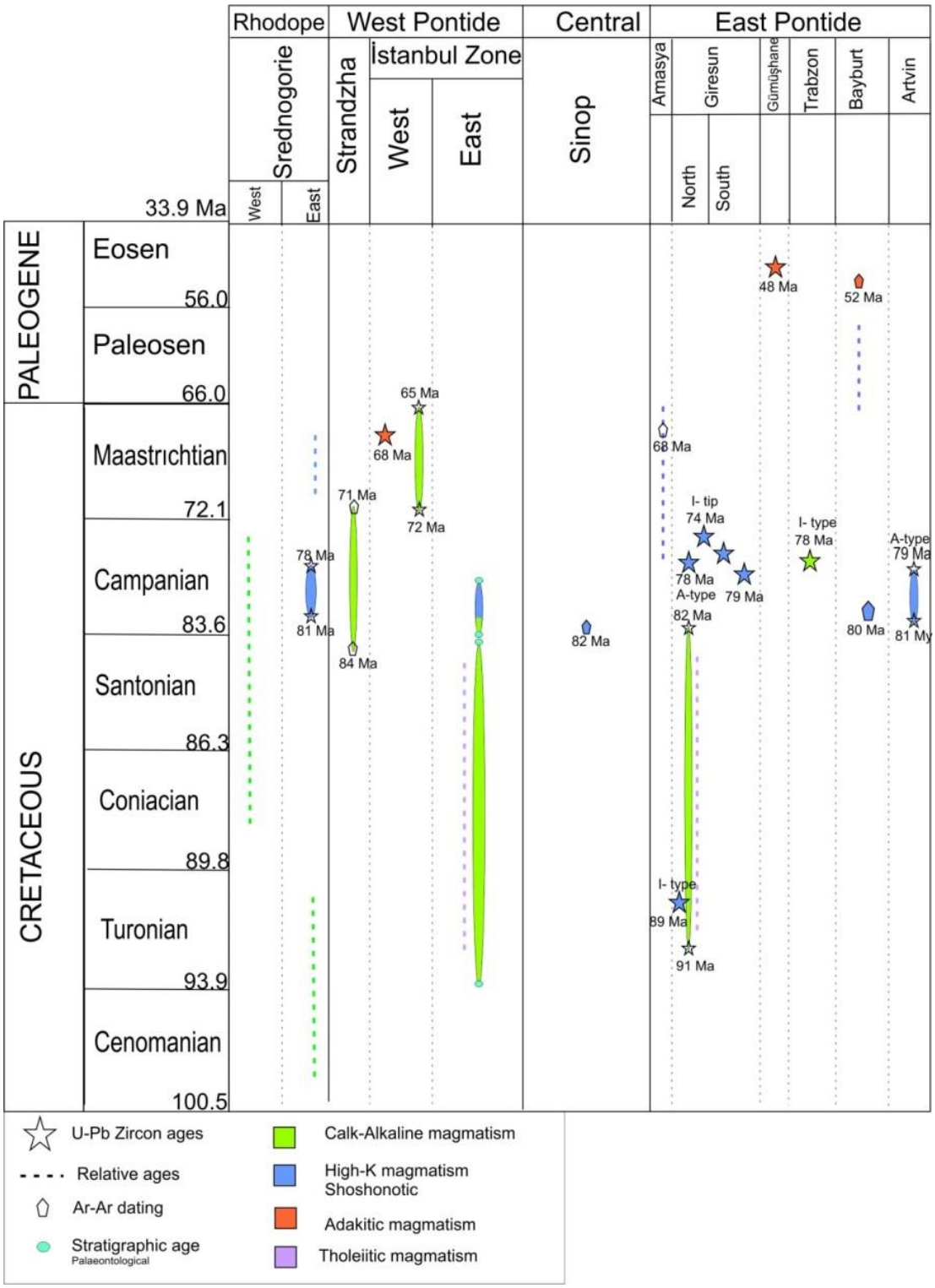

Figure 3. 7 : Age and geochemical data of Upper Cretaceous arc volcanism. Age data and geochemical analysis results are obtained Bocetti et al., 1978, Diker et al., 2008, Karacık and Tüysüz., 2009, Marchev et al., 2009, Eyüpoğlu., 2010, Speciale et al., 2012, Yılmaz Şahin et al., 2012, Kaygusuz et al., 2013, Asan et al., 2014, Aysal et al., 2018a, Keskin and Tüysüz., 2018, Boehm et al., 2019, Eyüboğlu et al., 2019.

3.3.1 Western Pontides

Upper Cretaceous volcanism occurred in two phases in the Eastern Sredna-Gora (Bulgaria) region. In the first phase, in the north of the East Sredna-Gora Zone, volcanism with calc-alkaline character is observed during the Cenomanian-Turanian period, Coniasian-Santonian is quiescent interval for volcanism in the eastern part of the Sredna-Gora Zone (Boccaletti et al., 1978, Marchev et al., 2009). Then a volcanism with shoshonitic character in the east of the East Sredna-Gora region is dominant in the Yambol region in the Bulgaria during the Campanian (81-78 Ma) period (Boccaletti et al., 1978, Marchev et al., 2009). In the west of Sredna-Gora zone, calc-alkaline volcanism developed during the Coniacian-Campanian period (Bocetti et al., 1978, Marchev et al., 2009). The Maastrichtien volcanism that developed in the second phase shows enrichment in K. Along the Sredna-Gora Zone, the Upper Cretaceous volcanism changes from west to east, from calc-alkaline character to high-K calc-alkali, shoshonitic and alkaline characters (Bocetti et al., 1978). In the Istranca zone, which is the eastern extension of the Apuseni–Banat—Timok–Sredna Gora belt, the Santonian- Maastrichtian (84-71 Ma) Demirköy Pluton has calc-alkaline character and is associated with subduction magmatism (Moore et al., 1980; Karacık and Tüysüz., 2012).

3.3.2 Eastern Pontides

In the Eastern Pontides, the 89 Ma old Dereli Granodiorite (Giresun), which cuts the pre-Upper Cretaceous volcano-sedimentary sequences and the basement metamorphics (Boynukalın, 1991, Eyüboğlu et al., 2018) has calc-alkaline character. During the Campanian, in Giresun region calc alkali I-type granites were developed in the northern part whereas K-rich and shoshonitic granites crop out in the south (Eyüboğlu et al., 2018). In Artvin, 78 Ma old A-Type granites are reported (Karslı et al.,2012, Eyüboğlu et al., 2018). The reason of such a variation in the magmatic characters was interpreted by Eyüboğlu et al. (2018) as the double-sided subduction of Paleotethys and Neotethys oceans during the Turonian-Early Campanian period. The late Campanian-Paleocene volcanics containing analcime enriched in K are also observed in Bayburt and Amasya regions (Eyüboğlu., 2010). Considering the geochemical features of the late Cretaceous arc belt, the calc-alkaline volcanism developed associated with subduction in the early stages of the late Cretaceous was

enriched in K during the Campanian- Maastrichtian period. This change in the character of magmatism has been interpreted by some researchers as a result of the opening of the Black Sea as a back-arc/intra-arc (Keskin at al. 2017, Karacık et al. 2019, Bocetti 1978, Boehm at al. 2019). Asan et al. (2014) interpreted the presence of shoshonitic and high-K volcanic rocks as subduction zone metasomatism and differentiation processes of magma occurred in shallow levels. We compared our geochemical results of the volcanic rocks with the ones in the Sredna-Gora Zone, the Strandja Zone, and the Eastern Pontide on the spider diagrams. According to the results of this comparison, geochemical feauters of the volcanic rocks outcropping along the Bulgarian Sredna-Gora Zone and the Eastern Pontides are different except that all show subduction sign. Incompatible elements of the volcanic rocks outcropping along the Bulgarian Sredna-Gora Zone, the Demirköy pluton in the Strandja Zone and the Eastern Pontides more enriched, while heavy rare earth elements of the volcanic rocks more depleted relative to the Riva volcanic rocks. However, the Demirköy pluton in the Strandja Zone is much similar than the Bulgarian Sredna-Gora Zone and the Eastern Pontides regions (Figure 3.8).

3.3.3 East of the İstanbul Zone

The late Cretaceous volcanism in the Istanbul Zone located just east of the Strandja and Sredna-Gora Zones similarly occurred in two different phases (Keskin et al., 2017, Tüysüz et al., 2011). In the first phase, the calc-alkali volcanism with subduction signature, which is thought to have been formed by the effect of the extensional tectonic regime in the east of the Istanbul Zone, continued throughout the Turonian-Santonian period (Keskin et al., 2003, 2010, Keskin et al., 2017, Boehm et al., 2019). The region was suddenly collapsed at end of the first phase in the Late Santonian and the volcanic rocks are unconformably overlain by shallow deep marine limestones (Tüysüz et al., 1999; Sunal and Tüysüz, 2002;). In the early stages of the second phase, the volcanism in the Campanian period has a calc-alkaline character. However, the volcanism transitioned to high K calc-alkaline, shoshonitic and alkaline volcanism in the late stages of the second phase (Keskin et al., 2017, Boehm et al., 2019). The volcanism has ended in the Maastrichtian period by the deposition of the Akveren Formation containing calciturbidite, limestone, clayey limestone and marl (Şahintürk and Özçelik, 1983; Tüysüz, 1999; Sunal and Tüysüz, 2002; Tüysüz et al., 2011) Limestones belonging to the Unaz Formation that divides

the volcanism into two in the east of the Istanbul Zone are not seen in the west of the Istanbul Zone. The Maastrichtyen aged (72-65 Ma) dyke, stock, and small-scale plutons cutting the Paleozoic and Upper Cretaceous sequences of the Istanbul Zone, show calc-alkaline character, except for a few samples with OIB character (Aysal et al., 2018a).

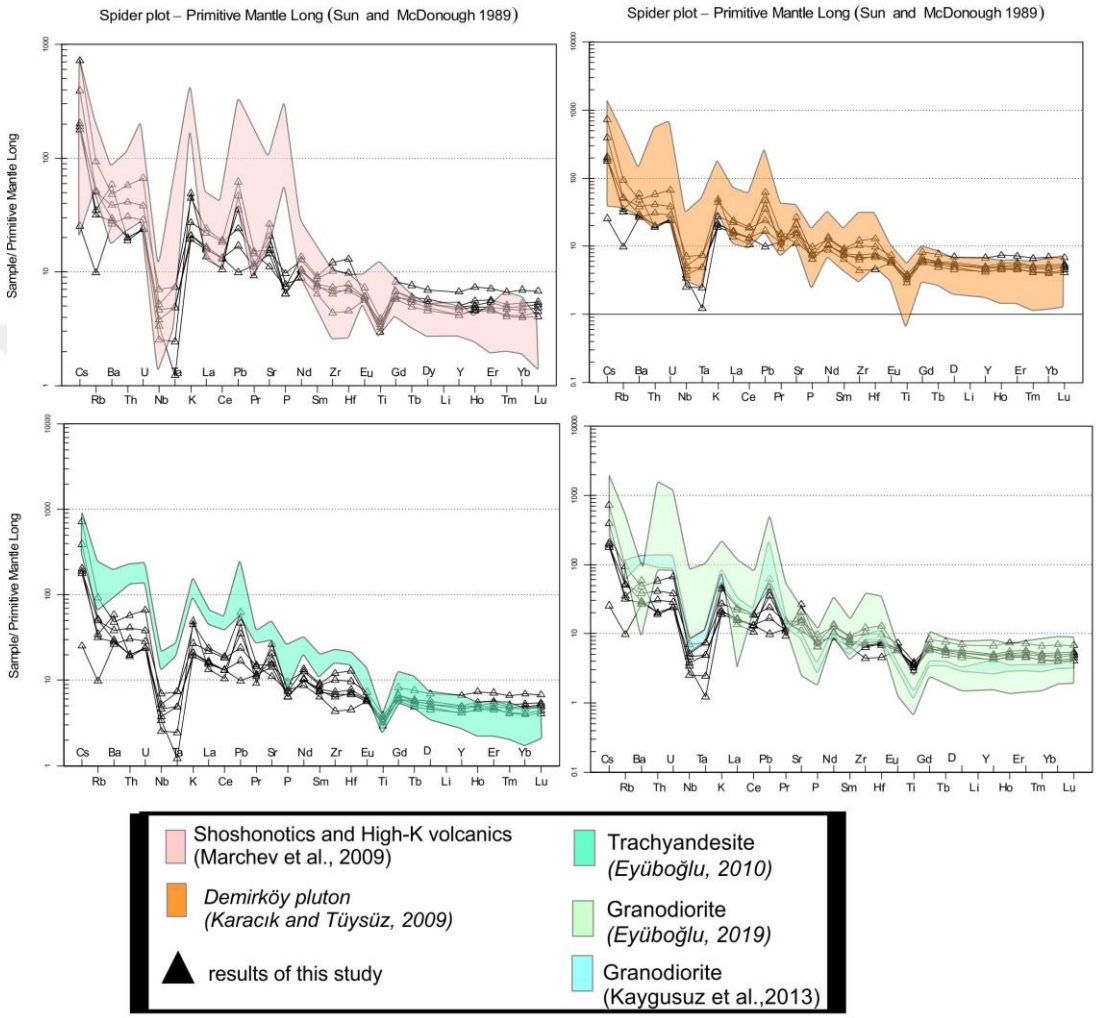

Figure 3. 8 : Primitive Mantle -normalized multi-element patterns a) Comparison of the geochemical analysis results of the volcanic rocks in the Sredna-Gora zone and this study on the spider diagram. b) Comparison of the geochemical analysis results of the volcanic rocks in the Strandzha zone and this study on the spider diagram. c-d) Comparison of the geochemical analysis results of the volcanic rocks in the Eastern Pontide and this study on the spider diagram.

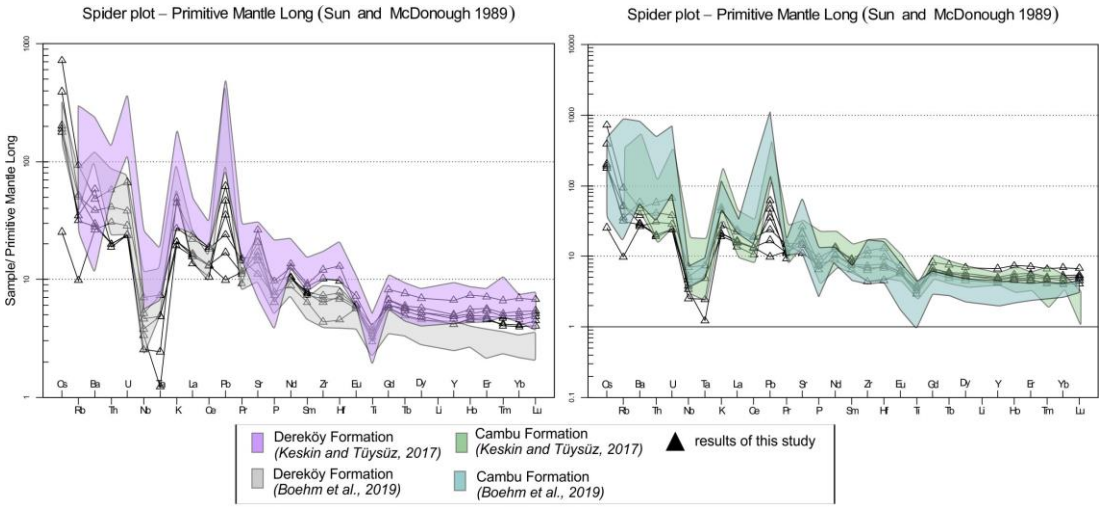

Figure 3. 9 : Primitive Mantle -normalized multi-element patterns a-b) Comparison of the geochemical analysis results of the volcanic rocks in the east of Istanbul Zone and this study on the spider diagram.

We compared the geochemical results of the volcanic rocks obtained in this study with the results published in the east of the Istanbul Zone on the spider diagrams. The results of this study are compatible with the analysis reported for the Dereköy and the Cambu Formations by Boehm et all (2019) and Keskin and Tüysüz (2018) (Figure 3.9).

3.4 The Intra-Continental Back Arc Systems

In this part, the geochemical analysis data of the Late Cretaceous volcanic rocks in the Istanbul Zone are compared with the volcanic rocks developed as a result of the intra-continental back-arc volcanism in well described regions on Earth.

In the study by Jiang (2017), the geochemical data collected from different regions interpreted as the intra-continental back arc were compared. As a result of these comparisons, it was determined that a typical inta-continental back-arc generally exhibits $(La/Yb)_N > 3$, Ba/La > 10 and Sm/Nd < 0.3 (Jiang et al., 2017). The results of our study exhibit La/Yb: 4.42-7.25 Ba/La: 16.40-43.87 Sm/Nd: 0.22-0.25.

Vasey et al. (2021) plotted data from 5 different intra-continental back-arc regions on the Th-3Tb-2Ta ternary diagram. The reason for using this diagram is that the incompatible Th, Ta and Tb elements have relatively different ratios to each other in different tectonic environments and therefore are useful in determining the geodynamic environment of the igneous rocks (Cabanis & Thieblemont, 1988;

Valset et al., 2021). We also plotted our results on the Th-3Tb-2Ta ternary diagram (Figure 3.10). Our analyses plotted mostly in an area where the geochemical data from the Okinawa Trough and the Shaquanzi Zone covers. Furthermore, all of the samples fell into the arc environment (Figure 3.10).

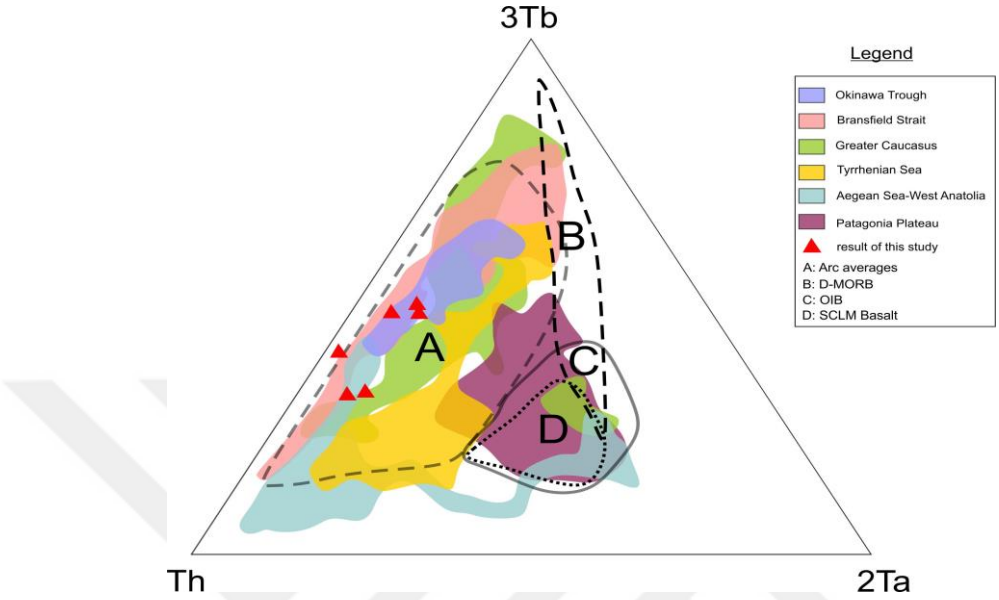

Figure 3. 10 : Th-3T-2Ta ternary diagram used for interpreting the geodynamic environment (Cabanis & Thieblemont, 1988; Vasey et.al.,2021).

In addition to that, results of our study and geochemical data from the Okinawa Trough and the Shaquanzi Zone, which were interpreted as intra-continental back arc were plotted on the spider diagrams. Primitive Mantle -normalized multi-element patterns of these regions exhibit close similarities with ours (Figure 3.11).

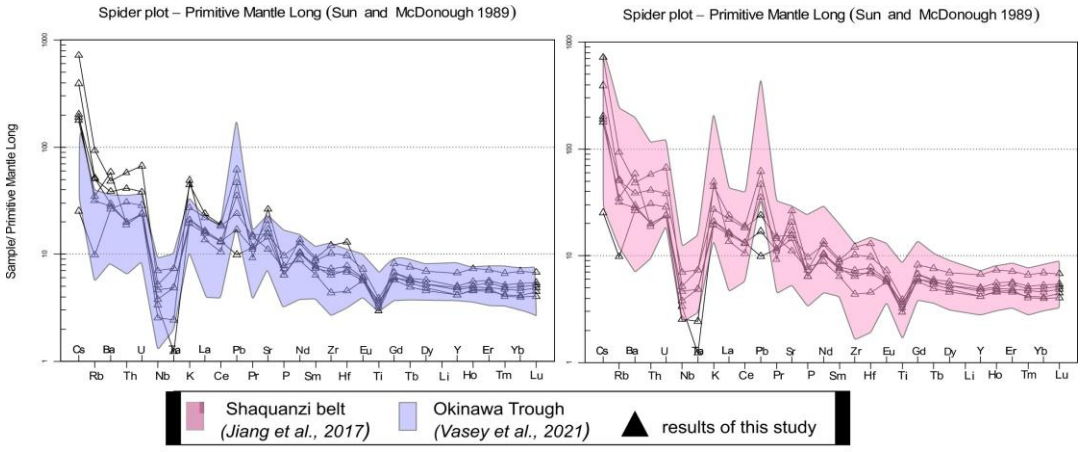

Figure 3. 11 : Primitive Mantle -normalized multi-element patterns a) Comparison of the geochemical analysis results of the volcanic rocks in the the Okinawa Trough region and this study on the spider diagram.b) Comparison of the geochemical analysis results of the volcanic rocks in the the Shaquanzi Belt and this study on the spider diagram.

3.5 Interpretation of the results

The volcanic rocks of the Riva Formation have basic and intermediate composition according to their % SiO_2 content. The negative Nb, Ta and Ti anomaly observed in the spider diagrams indicates that the magma has an orogenic character (Pearce, 1983, Rollinson, 1993).

Calc-alkaline nature of the rocks as revealed by the AFM diagram also supports subduction setting. Enrichment of magma with incompatible elements (Rb, Sr, Ba) may reflect crustal contamination. The deviation of Ce and Rb elements in spider diagrams may reflect hydrothermal decomposition (Bao and Zhao, 2008; Henderson, 1984).

In this study, two main separate comparisons were made. The first one, the spatial and temporal variation of the Upper Cretaceous volcanism in whole Pontides has been studied. The second one is a regional comparison with the known intracontinental back-arc basins studied on Earth. As a result of the first comparison, it can be stated that the calc-alkaline volcanism developed in relation to northward subduction of the Neo-Tethys oceanic lithosphere during the Turonian, and a reason passing into high-K calc-alkaline and shoshonitic magmatism is most probably of a progressive extentional tectonism occured during the Campanian. The second comparison was made to limit the geodynamic environment of volcanism in the Istanbul Zone. For this reason, the volcanic activity observed in the İstanbul Zone has been compared with the regions known as intra-continental back-arc tectonic environment. As a result, the volcanism studied in the İstanbul Zone may have formed in the early stages of an intra-continental back-arc environment. The similarity of geochemical data with Okinawa Trough and Shaquanzi regions supports this idea.

4. STRUCTRAL GEOLOGY

One of the main structural elements of the study area is the thrust fault called the Sarıyer-Şile fault. The fault is approximately 10 km long in the study area (Figure 4.1). The fault trends NW / SE and dips south (Kaya and Baykal, 1965; Baykal, 1943). The Paleozoic sedimentary sequence thrusted over the late Cretaceous volcanic sequence along the Şile thrust (Akartuna, 1963; Kaya and Baykal, 1965; Baykal, 1943). The Paleozoic units moved over the Upper Cretaceous units through the N-E direction (Kaya and Baykal, 1965; Baykal, 1943).

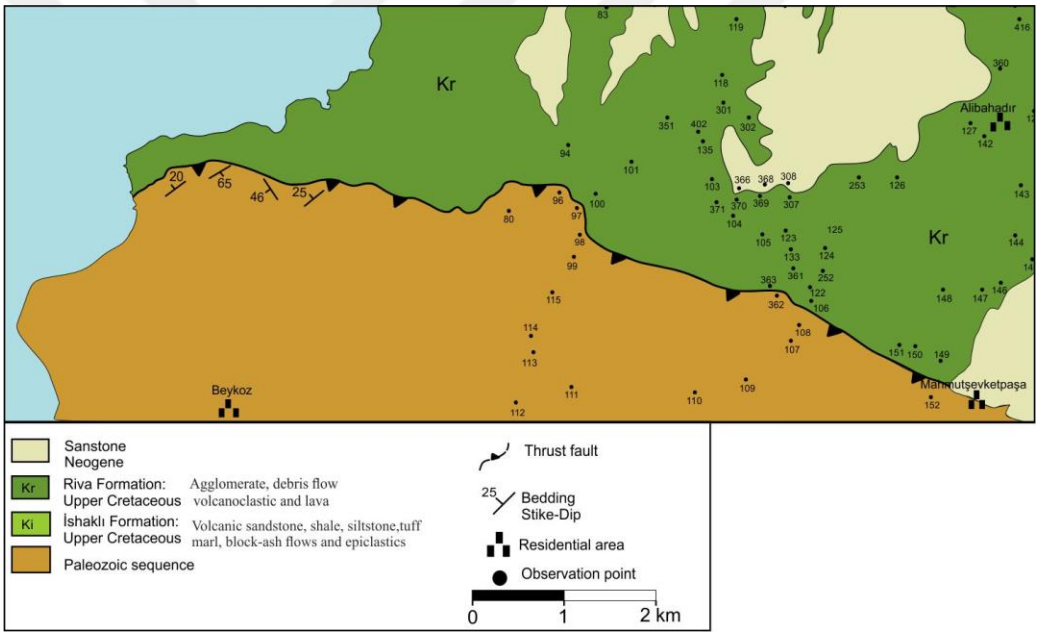

Figure 4. 1 : The Şile thrust observed in the study area.

Baykal (1943) stratigraphically determined the age of the fault as Ypresian-Lutetian as a result of his studies in the Şile region. While the Upper Cretaceous volcanic units in the study area show deformation, the Neogene sedimentary units are mostly subhorizontal. Therefore, the recommended age for the activity of the Şile thrust is compatible with the structural features of the rocks observed in the study area. Toward the fault plane, steepening of bedding and increasing in folding are observed in the Paleozoic sequence (Figure 4.2).

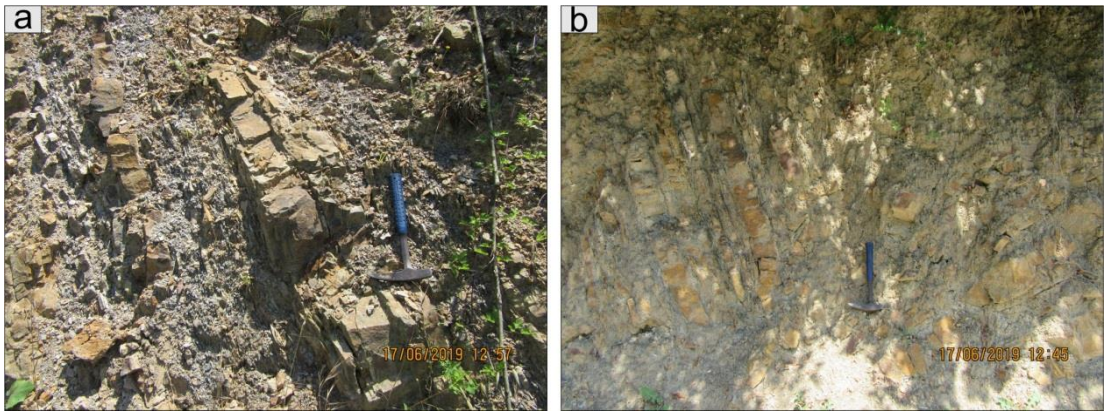

Figure 4.2 : Steepened sandstone-siltstone layers in the Paleozoic turbiditic sequence.

In the study area, a northward dip of 0-45^{o} is dominant in the turbiditic sequence of the İshaklı Formation. 26 bedding directions were measured from the İsaklı Formation. While 8 of them are inclined to NE direction, 14 of them are inclined to NW direction. The poles of the bedding planes were plotted on the stereographic projection (Figure 4.3). There is no significant folded in the İshaklı Formation but some minor fold observed in the study area (Figure 4.4).

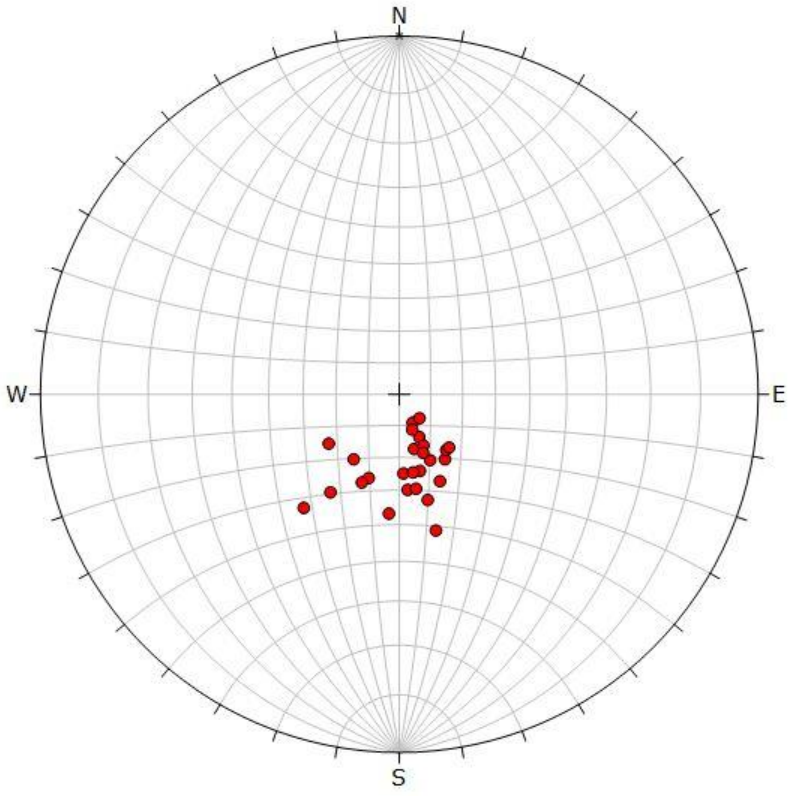

Figure 4.3 : The lower hemisphere stereographic projection. The poles of the bedding planes in İshaklı Formation.

Upper Cretaceous volcanic units are cut by syn-sedimentary normal faults and reverse faults (Figure 4.4). It indicates that the region was deformed during the deposition of the turbiditic sequence. Normal faults dominating the sequence may be the result of the extensional regime effect in the region.

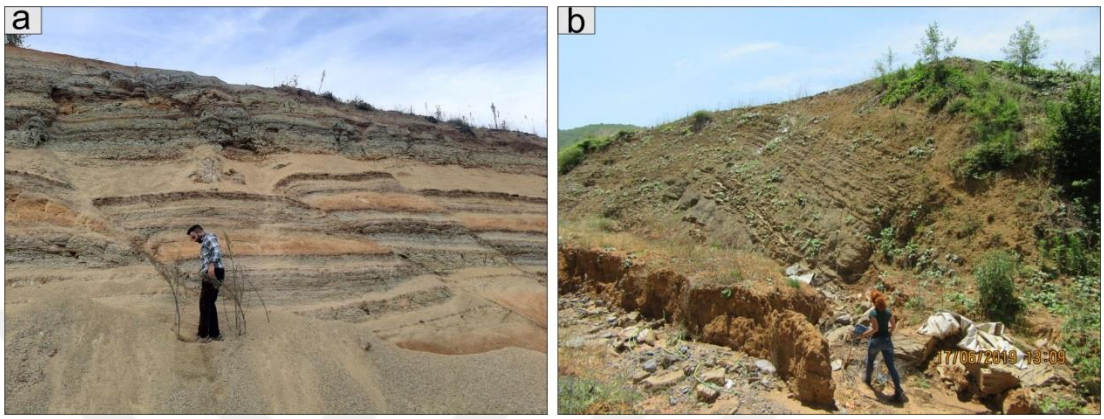

Figure 4.4 : a) Normal faults cutting the Upper Cretaceous sequence. b) Upper Cretaceous turbidite sequence folded as a result of deformation.

.

5. CONCLUSIONS

The results of this study can be listed as follows:

1) The volcanic unit in İstanbul Zone divided into two formations as the İshaklı and the Riva Formation. The İshaklı Formation consists of volcanogenic sandstone, shale, siltstone, marl, and epiclastic rocks. The İshaklı Formation is conformably overlain by the the Riva Formation which consist of volcaniclastics, tuffs, andesitic and basaltic lavas and agglomerates. The volcanic units are thrust over by the Paleozoic sedimentary sequence along the Eocene Sarıyer-Şile Thrust. All of the pre-Tertiary sequences are unconformably overlain by the terrestrial Neogene sediments.

2) LA-ICP-MS U-Pb dating was performed on zircon grains obtained from the tuff levels of the İsaklı and the Riva Formations. The age of the İshaklı and Riva formations was determined as 74.5 Ma (Campanian) and 78.56-76.3 Ma (Campanian), respectively.

3) Planktic foraminifera fossils were detect in the sandstones of the İsaklı Formation. These fossils are *Globotruncanita cf. elevata* (Brotzen), *Globotruncana cf. arca* (Cushman), and *Globigerinelloides sp.* The foraminifera assemblage yielded Campanian-Maastrichtian (possibly Campanian) age.

4) Geochemically, basalts and basaltic andesites of the Riva Formation are low-K calc-alkaline to medium-high K calc-alkaline rocks with magnesium numbers ranging from 32.6% to 51.5 %. The primitive mantle normalized spider diagram of trace elements show enrichment in LILE (K, Rb, Sr, Cs, Ba, Th and U) and depletion in HFS elements (Nb, Ta and Ti) . The high ratio of LILE/ HFS and negative Nb-Ta-Ti anomalies indicate that the volcanism evolved in a subduction setting (reference). Chondirite-normalized REE pattern display slight negative Eu anomalies and the La/Yb ratios of the samples range between 4.42-7.25.

5) In order to reveal spatial and temporal variation of late Cretaceous Arc volcanism and to reveal the geodynamic environment of the volcanism occurring in the Istanbul zone, the geochemical data obtained from previous studies were compared with the data of this study. As a result of comparisons, the character of the volcanism had a calc-alkaline character in the Turonian-Santonian period along the whole Upper

Cretaceous Volcanic belt, while the volcanism in the Campanian had high-K calc-alkaline and shoshonitic character in the Eastern Pontide. This change in the character of the volcanism may be related to the opening of the Black Sea basin as a back-arc basin during the Late Cretaceous.

6) The volcanism in the Istanbul Zone is geochemically similar to the Okinawa Trough and the Shaquanzi region, which are interpreted as intra-continental back-arc environment.

7) The age of the Dereköy formation, interpreted as the eastern equivalent of the İshaklı formation, was determined as Turonian-Santonian by the previous researchers. However, the planktic foraminifera assemblage determined from sandstones in the İshaklı Formation and the U-Pb zircon ages indicates that the succession was deposited in the Campanian period. It may have indicated that the volcanism is rejuvenated towards the west.

8) Our new geochemical, stratigraphical and the regional geological data suggest that north of the Istanbul Zone show a transition from fore-arc deposition to intra-arc volcanism during the Campanian time.

REFERENCES

Akartuna, M., (1963), Şile şariyajının İstanbul Boğazı kuzey yakalarında devamı. MTA Dergisi, **61**.

Akbayram, K., Okay, A.I., and Satır, M., (2013), Early Cretaceous closure of the Inta-Pontide Ocean in western Pontides (northwestern Turkey): *Journal of Geodynamics*, **65**, 38–55.

Akbayram, K., Şengör, A.M.C., and Özcan, E. (2016). The evolution of the IntraPontide suture: Implications of the discovery of late Cretaceous–early Tertiary mélanges. *The Geological Society of America Special Paper* 525, In Honor of Manuel Berberian's Forty-Five Years of Research Contributions.

Altınlı, İ. E., (1968), İzmit-Hereke-Kurucadağ alanının jeoloji incelemesi, *MTA Dergisi*., **71**, 10-16.

Asan, K., Kurt, H., Francis, D., & Morgan, G. (2014). Petrogenesis of the late Cretaceous K-rich volcanic rocks from the Central Pontide orogenic belt, North Turkey. Island Arc, **23**, 102–124.

Aysal, N., Keskin, M., Peytcheva, I., & Duru, O. (2018a). Geochronology, geochemistry and isotope systematics of a mafic–intermediate dyke complex in the İstanbul Zone. New constraints on the evolution of the Black Sea in NW Turkey. In: Simmons, M.D., Tari, G.C. and Okay, A.I. (eds.), *Petroleum Geology of the Black Sea. Geological Society, London, Special Publications*, **464**, 131-168.

Aysal, N., Sahin, S., Gungor, Y., Peytcheva, I., & Ongen, S. (2018b). Middle Permian–early Triassic magmatism in the Western Pontides, NW Turkey: Geodynamic significance for the evolution of the Paleo-Tethys. *Journal of Asian Earth Sciences*, **164**, 83-103.**Bao, Z. W., Zhao, Z. H.,** (2008). Geochemistry of Mineralization with Exchangeable REY in the Weathering Crusts of Granitic Rocks in South China. Ore Geology Review, **33**: 519–535.

Baykal, R, (1943), Geologie de la Region de Şile Kocaeli (Bithynie), Anatolie, *Istanbul Univ. Fen Fak. Monog.* No: 3, Istanbul.

Baykal, A.F. & Önalan, M., (1980). Şile sedimenter karışığı (Şile Olistostromu). *Altınlı Sempozyumu Kitabı, Türkiye Jeoloji Kurumu*, 15-25.

Boccaletti, M., P. Manetti, A. Peccerillo, G. Stanisheva-Vassileva. (1978). Late Cretaceous high-potassium volcanism in eastern Srednogorie, Bulgaria. *Geological Society of America Bulletin*, **89**, 439-447.

Boehm, K., Wagreich, M., Wolfgring, E., Tüysüz, O., Gier, S., & Yılmaz, İ. Ö. (2019). Upper cretaceous volcaniclastic complexes and calcareous

plankton biostratigraphy in the western pontides, NW Turkey. *Turkish Journal of Earth Sciences*, **28(2)**, 187–206.

Boynukalın, S., (1991). Dereli (Giresun) baraj yeri ve göl alanının mühendislik jeolojisi ve çevre kayaçlarının jeomekanik özellikleri (Doctoral dissertion). Karadeniz Technical University, Trabzon 128 pp. (in Turkish with English abstract).

Boynton, W. V. (1984). Cosmochemistry of the rare earth elements: meteorite studies. *Developments in geochemistry, Elsevier.* 2, 63-114.

Brotzen, F. (1934). Foraminiferen aus dem Senon Palästinas. *Zeitschrift des Deutschen Palästina-Vereins,* **57(1)**, 28-72.

Bürküt Y. (1966) Kuzeybatı Anadolu'da yeralan plütonların mukayeseli-jenetik etüdü. PhD thesis, İTÜ Maden Fakültesi, İstanbul, **272**.

Cabanis, B., & Thieblemont, D. (1988). La discrimination des tholeiites continentales et des basaltes arriere-arc; proposition d'un nouveau diagramme, le triangle Th-3xTb-2xTa. *Bulletin de La Societe Geologique de France,* **5(6)**, 927–935.

Chen F., Siebel W., Satır M., Terzioğlu N., & Saka K., (2002), Geochronology of the Karadere basement (NW Turkey) and implications for the geological evolution of the Istanbul zone. *Int. J. Earth Sci*, **91**, 469-481.

Cushman, J. A. (1926). The foraminifera of the Velasco Shale of the Tampico Embayment. *Bulletin of the American Association of Petroleum Geologist,* **10**, 581-612.

Dalbiez, F. (1955). The Genus Globotruncana in Tunisia. *Micropaleontology,* **1(2),** 161.

Diker, S., Çelik, M., & Kadıoğlu, Y. (2006). Finger prints of the formation of geothermal springs on the granitoids: BeypazarıAnkara, Turkey. *Environmental Geology*, **51**, 365–375.

Ercan, T., Türkecan, A., Guillou, Herve., Satır, M., Sevin, D., Şaroğlu, F., (1998). Marmara Denizi çevresindeki Tersiyer volkanizmasının özellikleri. *MTA Dergisi,* **120**, 199-221.

Eyuboglu, Y., (2010). Late Cretaceous high-K volcanism in the eastern Pontide orogenic belt: implications for the geodynamic evolution of NE Turkey. *Internatıonal Geology Revıew*, **52**, 142-186.

Eyuboglu, Y., Dudas, F. O. , ZHU, D., Liu, Z., & Chatterjee, N., (2019). Late Cretaceous I- and A-type magmas in eastern Turkey: Magmatic response to double-sided subduction of Paleo- and Neo-Tethyan lithospheres. *Lıthos*, **326**, 39-70.

Eyuboglu, Y., Dudas, F.O., Thorkelson, D., Zhu, D.C., Liu, Z., Chatterjee, N., Yi, K., Santosh, M., (2017). Eocene granitoids of northern Turkey: Polybaric magmatism in an evolving arc–slab window system. *Gondwana Research,* **50**, 311–345.

Gedik, İ., Duru, M., Pehlivan, Ş., & Timur E., (2005). Türkiye Jeoloji Haritaları İstanbul F22c Paftası**.** *M.T.A Jeoloji Etüdleri Dairesi.* No:11-13.

Georgiev, S., Marchev, P., Heinrich, C. A., Von Quadt, A., Peytcheva, and I., Manetti, P. (2009). Origin of nepheline-normative high-K ankaramites and the evolution of Eastern Srednogorie arc in SE Europe. *Journal of Petrology.*, **50(10)**, 1899-1933.

Green T. H., & Pearson, N. J., (1983) Effect of pressure on rare earth element partition coefficients in common magmas. *Nature*, **305**, 414–416.

Görür, N., (1988). Timing of opening of the Black Sea basin. *Tectonophysics*, **147**, 247-262.

Görür N., Monod O., Okay A. I., Şengör C., Tüysüz O., Yigitbas E., Sakinç M. & Akkök R., (1997). Palaeogeographic and tectonic position of the Carboniferous rocks of the western Pontides (Turkey) in the frame of the Variscan belt. *Bulletin de la Société géologique de France*, **168**, 197-206.

Irvine, T. N., & Baragar, W. R. A. (1971). A Guide to the Chemical Classification of the Common Volcanic Rocks. *Canadian Journal of Earth Sciences*, **8(5)**, 523–548.

İskenderoğlu, A., & Aysal, N. (2021). Chemo-stratigraphy, petrology and U-Pb geochronology of South-eastern part of the Yuntdağ volcano (Karakılıçlı – Manisa) in Western Anatolia. *All Earth*, ***33*(1)**, 30–51.

Jiang, H., Han, J., Chen, H., Zheng, Y., Lu, W., Deng, G., Tan, Z., (2017). Intra-continental back-arc basin inversion and late Carboniferous magmatism in Eastern Tianshan, NW China: Constraints from the Shaquanzi magmatic suite. *Geosci. Front*, **8**, 1447–1467.

Karacık, Z., and Tüysüz, O. (2010). Petrogenesis of the Late Cretaceous Demirköy Igneous Complex in the NW Turkey: implications for magma genesis in the Strandja Zone. *Lithos*, ***114*(3-4)**, 369-384.

Kaya, O., (1971). İstanbul'un Karbonifer Stratigrafisi. *Türkiye Jeoloji Kurumu Bülteni* **14**(**2)**, 143-199.

Kaygusuz, A., Sipahi, F., Ilbeyli, N., Arslan, M., Chen, B., & Aydınçakır, E. (2013). Petrogenesis of the Late Cretaceous Turnagöl intrusion in the eastern Pontides: Implications for magma genesis in the arc setting. *Geoscience Frontiers*, **4(4)**, 423–438.

Keskin, M., Ustaömer, T. ve Yeniyol, M., (2003). İstanbul kuzeyinde yüzeylenen Üst Kretase yaşlı volkano- sedimenter birimlerin startigrafisi, petrolojisi ve tektonik ortamı. İstanbul' un Jeolojisi Sempozyumu, Kadir Has Üniversitesi Cibali Kampüsü, 23- 35.

Keskin, M., Ustaömer, T., & Yeniyol, M. (2010). İstanbul kuzeyindeki Üst Kretase volkanojenik istiflerinin magmatik evrimi ve jeodinamik ortamı. *İstanbul'un Jeolojisi Sempozyumu III Kitabı*, 130-180.

Keskin, M., & Tüysüz, O. (2017). Stratigraphy, petrogenesis and geodynamic setting of Late Cretaceous volcanism on the SW margin of the Black Sea, Turkey. In: Simmons, M.D., Tari, G.C. and Okay, A.I. (eds.*), Petroleum Geology of the Black Sea. Geological Society, London, Special Publications*, **464**, 95-130.

Ketin, İ. (1966). Tectonic units of Anatolia. *Maden Tetkik ve Arama Bulletin*, **66**, 23–34.

Ketin, İ. ve Gümüş, A., (1963). Sinop-Ayancık arasında III. Bölgeye dahil sahaların jeolojisi. *Türkiye Petrolleri Anonim Ortaklığı*, Arşiv No. 288, Ankara (yayımlanmamış).

Le Bas, M. J., Le Maitre, R. N., Streckeisen, A., & Zanettin, B. (1986). A chemical classification of volcanic rock based on total silica diagram. *Journal Petrology*, **27(3)**, 745–750.

Marchev, P., Georgiev, S., Zajacz, Z., Manetti, P., Raicheva, R., von Quadt, A., &Tommasini, S. (2009). High-K ankaramitic melt inclusions and lavas in the Upper Cretaceous Eastern Srednogorie continental arc, Bulgaria: Implications for the genesis of arc shoshonites. *Lithos*, **113(1–2)**, 228–245.

McDonough, W. F., & Sun, S. s. (1995). The composition of the Earth. *Chemical Geology*, **120(3–4)**, 223–253.

Moore, W. J., Mckee, E. H. & Akıncı, Ö. (1980). Chemistry and chronology of plutonic rocks in the Pontid mountains, northern Turkey. *European Copper Deposits Congress Book*, 209–16. Belgrade.

Nelson, S.T & Montana, A. (1992) Sieved Textured Plagioclase in Volcanic Rocks Produced by Rapid Decompression. *American Mineralogist*, **77**, 1242-1249.

Okay, A.I., (2008) Geology of Turkey: A synopsis. *Anschnitt*, **21**, 19-42.

Okay, A.I., Satır, M. & Sıebel, W., (2006), Pre-Alpide orogenic events in the Eastern Mediterranean region. In: Gee, D.G. & R.A. Stephenson (eds.), European Lithosphere Dynamics. *Geological Society, London, Memoirs,* **32**, 389-405.

Okay, A.I., Şengör, A.M.C. & Görür, N. (1994), Kinematic history of the opening of the Black Sea and its effect on the surrounding regions. *Geology*, **22**, 267-270.

Okay, A.I. & Tüysüz, O., (1999), Tethyan sutures of northern Turkey. In "The Mediterranean Basins: Tertiary extension within the Alpine orogen" (eds. B. Durand, L. Jolivet, F. Horváth and M. Séranne), *Geological Society, London, Special Publication,* **156**, 475-515.

Önalan, M. (1982). Pendik Bölgesi ile Adaların Jeolojisi ve Sedimenter Özellikleri. (Doktora Tezi), İstanbul Üniversitesi (yayımlanmamış).

Özgül, N., (2012). Stratigraphy and Some Structural Features of the Istanbul Palaeozoic. *Turkish Journal of Earth Sciences,* **21**, 817–66

Öztunalı, Ö. & Satır, M. (1975). Rubidium-Strontium Altersbestimmungen des Tiefengesteinen aus Çavus¸bas¸ı (Istanbul). *İstanbul Üniversitesi Fen Fakültesi* Mecmuası, Seri B 40, 1–7.

Pearce, J. A., (1983). Role of the sub-continental lithosphere in magma genesisat active continental margins. In: C.J. Hawkesworth and M.J. Norry (Editors), Continental Basalts and MantleXenoliths. *Shiva publishing Ltd., Nantwich, Cheshire*. 230-249.

Pearce, J.A. (2008) Geochemical Fingerprinting of Oceanic Basalts with Applications to Ophiolite Classification and the Search for Archean Oceanic Crust. *Lithos,* **100**, 14-48.

Pearce, J. A. and Peate, D. W., (1995). Tectonic implications of the composition of volcanic arc magmas. *Ann. Rev. Earth Planet Sci*., **23**, 251-285.

Peccerillo, A., & Taylor, S. R. (1976). Geochemistry of eocene calc-alkaline volcanic rocks from the Kastamonu area, Northern Turkey. *Contributions to Mineralogy and Petrology*, **58(1)**, 63–81.

Penck, W., (1919). Grundzüge der Geologie des Bosporus. Veröff. des Instit. für Meereskunde, *Geol. Naturw. Reihe*, H. **4**, Berlin.

Rollinson, H., (1993). Using Geochemical Data: Evaluation, presentation, interpretation. *Longman Scientific and Technical* Group, New York, 352.

Sayar, C., (1979). İstanbul Boğazı ve çevresinde Ordovisyen-Siluriyen sınırı. *Türkiye Jeoloji Kurumu bülteni*, **22**, 161-167.

Speciale, P. A., Catlos, E. J., Yıldız, G. O., Shin, T. A., & Black, K. N. (2014). Zircon ages from the Beypazarı granitoid pluton (north central Turkey): Tectonic implications. Geodinamica Acta, **25**, 162–182.

Sunal, G., & O. Tüysüz (2002), Palaeostress analysis of Tertiary postcollisional structures in the western Pontides, northern Turkey, Geol. Mag., **139**, 343–359.

Şahintürk, O. ve Özçelik, Y., (1983). Zonguldak- Bartın-Amaşra-Kurucaşile-Cide dolay- larının jeolojisi ve petrol olanakları. *Türkiye Petrolleri Anonim Ortaklığı*, Rapor No. 1816, Ankara (yayımlanmamış).

Şengör, A. M. C., & Yılmaz, Y. (1981). Tethyan evolution of Turkey: A plate tectonic approach. *Tectonophysics*, **75**, 181–241.

Tüysüz, O., (1999**),** Geology of the Cretaceous sedimentary basins of the Western Pontides. *Geological Journal*, **34**, 75-93.

Tüysüz, O., Yılmaz, İ.Ö., Svabenıcka, L.&Kırıcı, S. (2012). The Unaz formation: a key unit in the Western Black Sea region, N Turkey. *Turkish Journal of Earth Sciences*, **21**, 1009–1028.

Ustaömer, P.A., Mundil, R., & Renne, P.R., (2005), U/Pb and Pb/ Pb zircon ages for arc-related intrusions of the Bolu Massif (W Pontides, NW Turkey): Evidence for Late Precambrian (Cadomian) age: *Terra Nova*, **17**, 215–223.

Vasey, D. A., Cowgill, E., & Cooper, K. M. (2021). A preliminary framework for magmatism in modern continental back-arc basins and its application to the Triassic-Jurassic tectonic evolution of the Caucasus. Geochemistry, Geophysics, Geosystems, **22**, 330-362.

Winchester, J. A., & Floyd, P. A., 1977. Geochemical discrimination of different magma seriesand their differentiation products using immobile elements: *Chemical Geology*, **20**, 325-343.

Yavuz,O.,. (2008) İstanbul kuzeyi volkanitlerinin jeolojik ve petrolojik incelenmesi, İstanbul Teknik Üniversitesi, Doktora Tezi.

Yeniyol, M., & Ercan, T., (1989-1990). İstanbul Kuzeyinin Jeolojisi, Üst Kretase volkanizmasının petrokimyasal özellikleri ve Pontidlerdeki Bölgesel Dağılımı, *İ.Ü.Müh. ak. Yerbilimleri Dergisi*, **7(1-2)**, 125-147.

Yılmaz İ., (1977), Absolute age and genesis of the Sancaktepe granite (Kocaeli peninsula). *Bulletin of the Geological Society of Turkey*, **20**, 17-20.

Yılmaz-Şahin S., Aysal N., Güngör Y. & Öngen S. (2010). Petrogenesis and shrimp zircon U-Pb dating of some granitoids within the western Pontides, southeastern Balkans, NW Turkey. *XIX Congress of Carpathian-Balkan Geological Association*, Thessaloniki, Greece, 23-26 September.

Yılmaz-Şahin, S., Aysal, N., & Güngör, Y. (2012). Petrogenesis of Late Cretaceous adakitic magmatism in the Istanbul Zone (Çavuşbaşı Granodiorite, NW Turkey). *Turkish Journal of Earth Sciences,* **21(6)**, 1029–1045.

Yiğitbas, E., Kerrıch, R., Yılmaz, Y., Elmas, A., & Xıe, Q., (2004). Characteristics and geochemistry of Precambrian ophiolites and related volcanics from the Istanbul-Zonguldak Unit, Northwestern Anatolia, Turkey: following the missing chain of the Precambrian South European suture zone to the east. *Precambrıan Research* , **132**, 179-206.

Yurtsever, A., (1982), Kocaeli Triyası Biyostratigrafi Projesi, Gebze-Hereke Tepecik alanında Mesozoyik-Senozoyik kayalarının jeolojisi. MTA Raporu *No.7195,* Ankara (yayımlanmamış).

CURRICULUM VITAE

Name Surname : Cemre Ay

EDUCATION

▪ **B.Sc. :** 2018, İstanbul University, Faculty of Mines,
Geological Engineering Department

PROFESSIONAL EXPERIENCE AND REWARDS:

▪ **2019 - :** Research assistant at, Faculty of Mines, Department of Geological Engineering, İstanbul Technical University.

PUBLICATIONS AND PRESENTATIONS

▪ Ay C., Sunal G., Okay A.I., Upper Cretaceous Stratigraphy and Volcanism in the Igneada Region, Pontides, NW Turkey, EGU 2021 – General Assembly.